SOUTHEASTERN

GEOLOGY

This journal welcomes original papers on all phases of geology, geophysics, and geochemistry as related to the Southeast. Transmit manuscripts to S. DUNCAN HERON, JR., BOX 6665, COLLEGE STATION, DURHAM, NORTH CAROLINA. Please observe the following:

(1) Type the manuscript with double space lines and submit in duplicate.
(2) Cite references and prepare bibliographic lists in accordance with the method found within the pages of this journal.
(3) Submit line drawings and complex tables as finished copy.
(4) Make certain that all photographs are sharp, clear, and of good contrast.
(5) Stratigraphic terminology should abide by the Code of Stratigraphic Nomenclature (AAPG, v. 45, 1961).

Proofs will not be sent authors unless a request to this effect accompanies the manuscript.

Reprints must be ordered prior to publication. Prices are available upon request.

* * * * * *

Subscriptions to Southeastern Geology are $5.00 per volume. Inquiries should be addressed to WM. J. FURBISH, BUSINESS AND CIRCULATION MANAGER, BOX 6665, COLLEGE STATION, DURHAM NORTH CAROLINA. Make check payable to Southeastern Geology.

SOUTHEASTERN GEOLOGY

Table of Contents

Vol. 10, No. 3

1969

THE NATURE OF GRANODIORITE UNDER TRIAXIAL STRESS

AND A POSSIBLE MODEL FOR SEISMIC DISTURBANCES

By

A. A. Giardini
Department of Geology
University of Georgia

ABSTRACT

Experimentally determined failure data for granodiorite under triaxial compressive stress are reviewed. Two distinct modes of failure are observed to alternately occur with increasing mean confining stress. They are brittle shear-characterized by an audible shock and a relatively quiet slip shear. A failure diagram is constructed on the basis of available experimental data to a mean confining stress of 60 kilobars. When considered in terms of equivalent terrestial depth, a correlation is found between the failure model and the pattern of terrestial seismic activity. A speculative extrapolation to higher stress levels continues to show an apparent correspondence with the seismic characteristics of the earth. Hypothetical strain release energies calculated for a subsurface 50 x 10 kilometer fracture in accordance with the model show agreement with reported strain release energies of earthquakes. If the failure model, which is presently based only on the failure characteristics of granodiorite, can be shown to be of general applicability for subsurface igneous rock, then it may provide a framework for developing an approximate capability to predict a future earthquake in a region with a well-documented history of preceding earthquakes.

INTRODUCTION

Seismic records indicate that more than one million earthquakes occur each year (Hodgson, 1964). About a thousand are of sufficient intensity to cause serious damage. Of these, ten to twenty usually occur in populated areas with results that are often devastating. Hundreds of thousands of lives and billions of dollars in property are known to have been lost to earthquakes (Hodgson, 1964).

Research during the past several decades has yielded some understanding of the general nature of the earth's interior, and also the ability to quickly locate the focus and epicenter of an earthquake. The ability to predict occurrence, however, has remained essentially zero.

The model described here appears to have the potential for developing a reasonable capability to statistically predict a future earthquake where previous ones have occurred. Examples considered are land masses with adjoining ocean deeps. At present the model must be considered as speculative since it is based solely on the relationship observed between the nature of sequential earthquakes at the above localities and the experimentally determined failure characteristics under increasing triaxial stress of a single rock, granodiorite. However, a few semi-quantitative experiments on basalt indicate a behavior similar to granodiorite.

The underlying assumption upon which the model currently rests is that granodiorite, being a brittle igneous rock, possesses failure characteristics under triaxial stress that are reasonably consistent with those of other igneous rocks. No implication is intended that the earth's internal petrology where earthquakes originate is granitic. The choice of granodiorite for the experimental work was not originally related to a study of earthquakes.

At present there is insufficient suitable failure data on other rocks to determine the validity of the assumed generality of failure characteristics. However, no inconsistencies between observed seismic characteristics of the earth and the proposed rock failure model have been encountered thus far. The model is given in its present tentative state in the hope that it may be of interest to others working in this area of research.

A Brief Review of the Material Tested

The rock came from the Atomic Energy Commission Nevada Test Site, and is commonly called Hardhat granite. Actually it is a medium-grained granodiorite with the following average mineralogical composition:

quartz	= 28.6 percent by volume
orthoclase feldspar	= 22.5
calcic andesine feldspar	= 37.4
biotite mica	= 6.5
hornblende amphibole	= 0.1
iron sulfides and oxides	= 0.8
sphene	= 0.4
apatite	= 0.1
water	= 1.0 ± 0.4

In bulk, the rock was generally fractured, with the fine seams often filled with the following alteration products:

chlorite	= 0.7 percent by volume
penninite	= 0.6
sericite	= 1.4
kaolinite	= 0.8
epidote	= 0.08

Veinlets of pyrite crystals also were encountered from time to time. The average grain size of the rock was about 0.8 mm, with observed limits ranging from about one centimeter to microns.

Samples of rock were taken from various depths by drill core down to approximately 300 meters prior to the detonation of a 5.0$\pm$ 1.0 kiloton nuclear device located at a depth of 290 meters. Subsequent to the explosion, samples were taken 23 and 27.5 meters from ground zero. The petrological and physical details of the rock before and after the explosion have been reported by Short (1966).

Samples for triaxial compression tests were cut at 0°, 45° and 90° to the drill core axis and ground to right circular cylinders 2.54 cm long and 1.27 cm in diameter. All specimens were tested in the "as received" condition. In addition to the pre- and postdetonation samples, a number of the predetonation specimens were mechanically shattered in the laboratory, recompacted, and subjected to the triaxial compression tests.

Specimens were jacketed in annealed thin-walled copper tubes in order to prevent penetration of the confining pressure fluid (low viscosity oil) into the rock. Experiments were carried out in a piston-cylinder apparatus. Specimens were first subjected to a given confining pressure, and then a longitudinal stress was imposed until the rock failed. As the longitudinal stress increased, the confining pressure also increased. The longitudinal stress was measured with an internal strain gauge, and the confining oil pressure was measured with an internal manganin coil gauge. The observed failure in all experiments under confining pressure was by shear. All specimens remained elastic prior to defined failure. Details of the experimental apparatus, technique and data have been published elsewhere (Giardini et al., 1968).

<center>A Brief Review of the Coulomb Shear Stress Theory and a
Modified Coulomb Equation for this Work</center>

The stress system in terms of orthogonal coordinates is illustrated by Figure 1. The term S_p represents the confining fluid pressure, and

$$S_p = S_2 = S_3. \qquad\qquad 1.$$

The term S_c represents the mechanically superimposed longitudinal stress, and is sometimes referred to as the longitudinal stress difference. The total longitudinal stress is equal to S_1, where

$$S_1 = S_c + S_3. \qquad\qquad 2.$$

The shear stress on the specimen at failure is referred to as the maximum shear stress. It is designated by T_M and is equal to

$$T_M = \frac{S_1 - S_3}{2} = \frac{S_c}{2}. \qquad\qquad 3.$$

Under compression, the angle between the longitudinal stress direction and the failure plane is designated as θ. The stress component normal
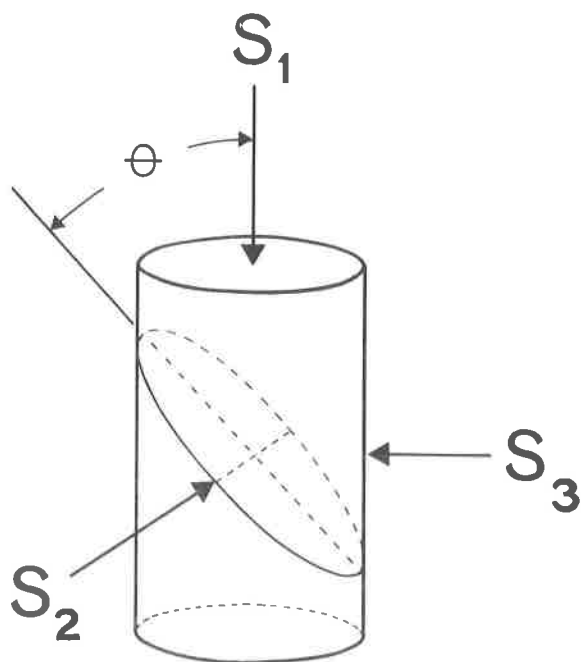
<center>127</center>

Figure 1. The triaxial compressive stress
field upon the cylindrical test specimens.

to the failure plane is given by

$$S_n = \frac{S_1 + S_3}{2} - \frac{S_1 - S_3}{2} \cos 2\theta. \qquad 4.$$

In terms of the two dimensional Coulomb theory of internal fric-
tion (Coulomb, 1776, and Mohr, 1882 and 1900), the shearing resis-
tance of an isotropic material to failure can be considered as the sum
of a directionally independent fundamental cohesive shear strength, T_0,
plus a term which represents resistance to sliding friction along the
failure plane. The frictional term is given by the product of a coeffi-
cient of internal friction and the stress normal to the failure plane.
The Coulomb shear stress for failure is given by the equation,

$$T = T_0 + S_n \tan \Phi. \qquad 5.$$

The term $\tan \Phi$, sometimes also given as n, represents the coeffi-
cient of internal friction. The angle Φ is related to the angle of in-
clination of the failure plane according to

$$\Phi = \pm 45° \pm \frac{\theta}{2}. \qquad 6.$$

Goranson (1940) has given an explanation of the significance of θ.
For the three dimensional case of this work, the Coulomb

128

expression has been modified so as to consider the mean confining stress, defined by

$$S_m = \frac{S_1 + S_2 + S_3}{3},$$ 7.

and the previously defined maximum shear stress upon the specimen. The modified Coulomb maximum shear stress equation used in this work is

$$T_M = T_o + S_m \tan \Phi.$$ 8.

The experimental data on granodiorite failure under triaxial stress are found to comply with the above expression.

THE EXPERIMENTAL DATA

A summary of the observed experimental data is given in Figure 2 in terms of the maximum shear stress on the specimen, T_M, and the mean confining stress, S_m, at failure. Approximately 50 successful experiments are represented. Triangles represent brittle shear failures which occurred instantaneously and with an audible bang. Circles indicate quiet slip shear failures. Undarkened symbols represent unshocked granodiorite, and darkened symbols are for rock specimens which were subjected to shock either by the subsurface nuclear detonation (about 20 kilobars peak stress), or by mechanical means in the laboratory (about 35 to 40 kilobars peak stress).

It is interesting to note that the granodiorite shocked by nuclear detonation, although permeated with fine fractures, was still mechanically coherent and possessed a compressive strength at atmospheric pressure of about half that of unshocked material. The mechanically shocked rock was reduced essentially to loose grains and had to be jacketed in thin wall lead tubes and recompacted to a cylindrical shape in order to carry out the triaxial tests.

No effects were observed in the failure of the specimens which could be related to orientation relative to the drill core axis, nor with respect to variation in mineralogical composition or texture. No attempt was made to control the as-received water content of the specimens.

Under confining pressure, the behavior of all shocked specimens converged to that of unshocked rock. Longitudinal strain measurements made in conjunction with the triaxial failure tests showed that under confining pressure the specimens remained elastic to a point just preceding rupture. The experimental evidence seems to indicate, therefore, that within the limits encountered the rock behaves essentially isotropic and independent of its physical state when under confining pressure.

As indicated above, two modes of failure were observed under confining pressure. One was an instantaneous brittle shearing rupture which produced a bang. The other was a relatively quiet more gradual
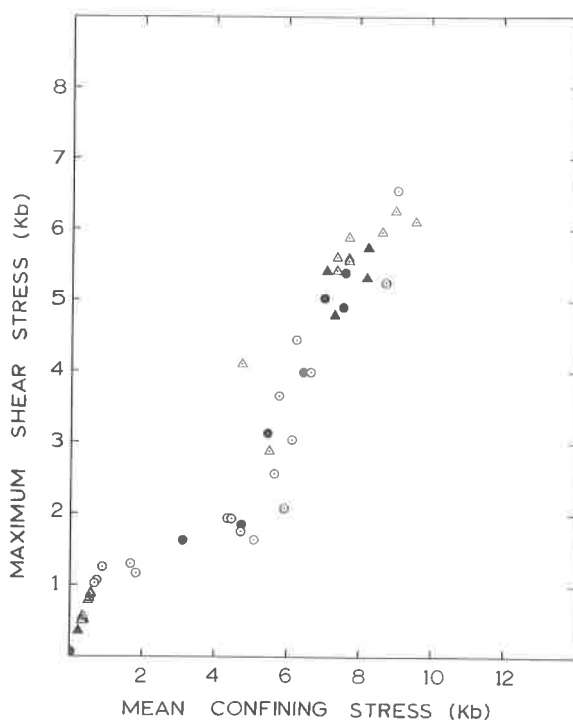
Figure 2. Observed points of granodiorite
failure by shear under triaxial compres-
sive stress. Open triangles represent
normal specimens which failed by brittle
shear. Dark triangles are for preshock-
ed material which failed by brittle shear.
Open circles designate normal rock which
failed relatively quietly by a slip shear.
Dark circles are for preshocked material
which sheared quietly.

shear failure. The only difference observed between the rupture sur-
faces from the two modes of failure was that brittle failure produced a
fine fault gouge whereas quiet slip failure yielded coarser mineral frag-
ments. The respective brittle and quiet slip failure data are plotted
separately in Figures 3 and 4. The lines represent the statistical
linear slopes evaluated with respect to the modified Coulomb equation.

The initial leg of the brittle failure curve shown in Figure 3 re-
presents tests performed at atmospheric confining pressure. The
equation for this segment is

$$T_M = 0.1 + 1.42 \ (\pm 0.02) \ S_m, \qquad\qquad 9.$$

with $0 \leqslant S_m \leqslant 0.74$ kilobars. The numbers are averages determined
with the aid of a computer. The standard deviation is indicated in the
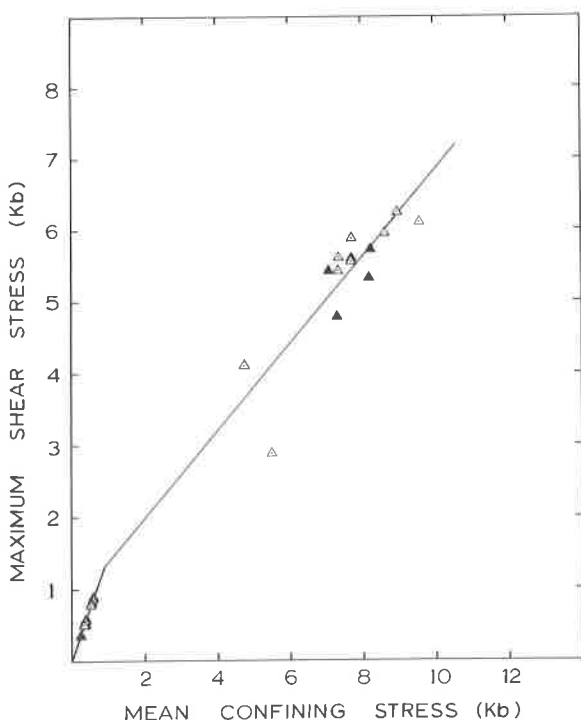
130

Figure 3. Distribution and slopes for brit-
tle shear failures. The initial slope at
atmospheric confining pressure is 1.425.
Under confining pressure, the slope is
0.59.

bracket. The T_O value for the atmospheric tests was determined
separately by torsion tests. The upper segment of the curve for brittle
failures is described by

$$T_M = 0.81 + 0.59 \ (\pm 0.09) \ S_m,$$ 10.

with $0.74 \leqslant S_m \leqslant ?$ kilobars.

With respect to the quiet shear failures of Figure 4, the first
segment of the diagram coincides with that of the atmospheric brittle
failures. The tests represented here are those performed on speci-
mens which were severely preshocked by mechanical means in the
laboratory. The second segment of the quiet slip failure data is des-
cribed by the equation,

$$T_M = 1.0 + 0.17 \ (\pm 0.04) \ S_m,$$ 11.

with $0.74 \leqslant S_m \leqslant 5.78$ kilobars. The equation of the third leg is

$$T_M = -3.5 + 1.14 \ (\pm 0.6) \ S_m,$$ 12.

with $4.7 \leqslant S_m \leqslant 7.9$ kilobars. This segment intersects with the brittle
failure curve (equation 10) at the mean confining stress value $S_m = 7.9$
kilobars, and appears to represent a transitional state between the slip

131
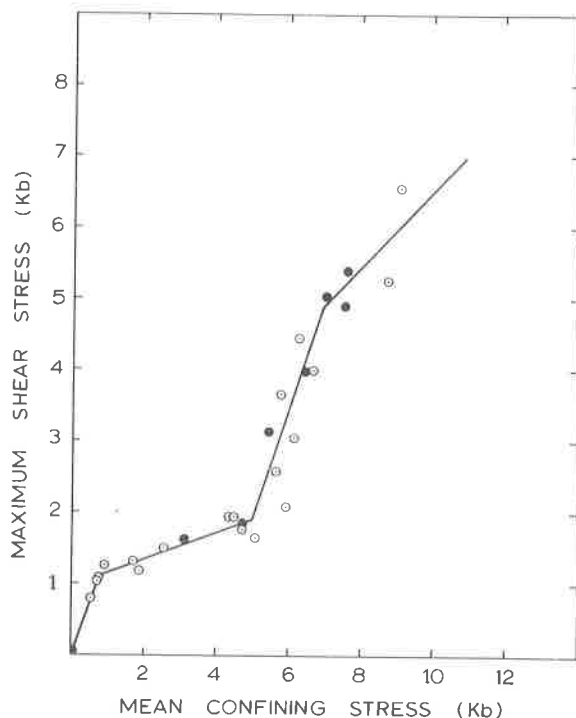
Figure 4. Distribution and slopes for re-
latively quiet slip shear failures. The
initial slope at atmospheric confining
pressure is 1.425. The slope of the
second section of the curve is 0.17.
The slope of the third segment is 1.135,
and that of the uppermost segment is
0.59.

and brittle modes of failure. It is within this segment of the failure
curve that the Young's modulus of preshocked rock showed convergence
to that of unshocked material (Giardini et al, 1968).

The curves for the observed modes of failure and respective
slopes are summarized in Figure 5. The slopes of the respective seg-
ments of the failure diagram are equivalent to the Coulomb coefficient
of internal friction. All segments of the failure data show agreement
with the modified Coulomb maximum shear stress expression.

DISCUSSION OF THE EXPERIMENTAL DATA

A study of the literature revealed no previous report of a re-
latively quiet slip type of shear failure for granitic rock. As mentioned

132
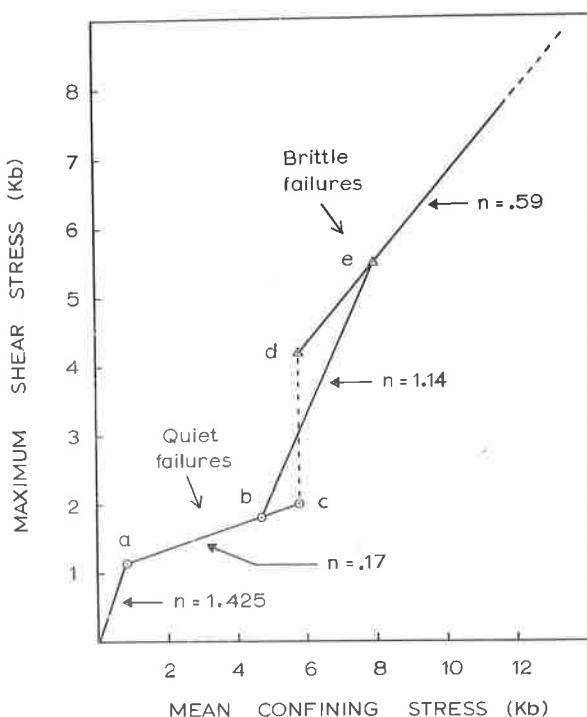
Figure 5. The averaged failure curves for
all experiments. The slopes, n, are
equivalent to the Coulomb coefficient of
internal friction. The initial mode of fai-
lure is brittle shear. It is followed by a
region of relatively quiet slip shear,
which in turn, at higher stresses, is fol-
lowed by a second region of brittle shear
failure. Letters pertain to discussion in
the text.

earlier, strain measurements showed adherence to Hooke's law to a
point preceding failure. No residual barrelling or other evidence sug-
gestive of plastic deformation or "ductile flow" was observed on any of
the specimens. With few exceptions, failure under confining pressure
occurred by a single shear surface inclined about 30 degrees to the
principal axis. These experiments, however, were of short duration,
and over long periods of time granodiorite may behave differently. The
interrelationship between the inclination of the rupture surface and the
rate of stress application is discussed by Goranson (1940). Figure 5,
therefore, specifies a short term limiting average triaxial stress field
for mechanical stability, or conversely, failure by shear of granodio-
rite.

133

At present there is no explanation for the observed region of relatively quiet slip failure. There are two conditions, however, which might account for its occurrence. First, consider the existence of appreciable essentially two dimensional free space (pore space) in the rock in the form of an extensive network of fine fractures. Both the normal and the preshocked rock possessed such networks of fractures, with a greater severity in the latter. This free space reduces the coherency of the rock as evidenced by the lower compression strength of preshocked specimens. It also may constitute the defect responsible for the observed slip mode of failure.

A theoretical analysis of pore collapse by Walsh (1965) has shown that the pressure required to close shallow elliptical pores is approximately given by

$$P_C = E r, \qquad\qquad 13.$$

where P_C is the critical pressure for collapse, E is Young's modulus for the material, and r is the average axial ratio for shallow elliptical cracks. Stephens and Lilley (1966) have found the axial ratio to be of the order of 10^{-3} for Hardhat granite, and have experimentally shown that the very extensive network of fractures produced in this rock by a mechanical shock of about 40 kilobars closes at about 3 kilobars of confining pressure.

A review of the experimental data of this study in terms of T_M and confining pressure, P, rather than mean confining stress, is given in Figure 6. It shows that the slip mode of failure terminates for all classes of rock tested in the range 3 to 4 kilobars of confining pressure. This is in satisfactory agreement with the work of Walsh and that of Stephens and Lilley.

Should a film of fluid exist on the internal free surface, the so-called pore effect could be further affected either or both by the possible generation of an entrapped pore pressure which could act counter to the stress component normal to the potential failure plane, and by any lubricating influence the fluid might have on the sliding friction of the material.

The effect upon the maximum shear stress which a possible pore pressure could have is illustrated by the equation of Handin et al (1963),

$$T = T_0 + (S_n - p), \qquad\qquad 14.$$

where S_n is the stress component normal to the failure plane and acting to prevent failure, and p is the pore pressure acting against it. It is clear that if a pore fluid were entrapped in the cracks it could contribute to a reduced value of T_M for failure.

Second, consider the failure data according to modified Coulomb criteria. The following behavior is suggested. Subsequent to rupture in the region of slip shear failure, sliding will occur along the failure surfaces as long as the shear component of stress exceeds the frictional component. This is given by

$$T_M - T_0 > n S_m. \qquad\qquad 15.$$

At point c and beyond (Figure 5), where the fractures are closing, the
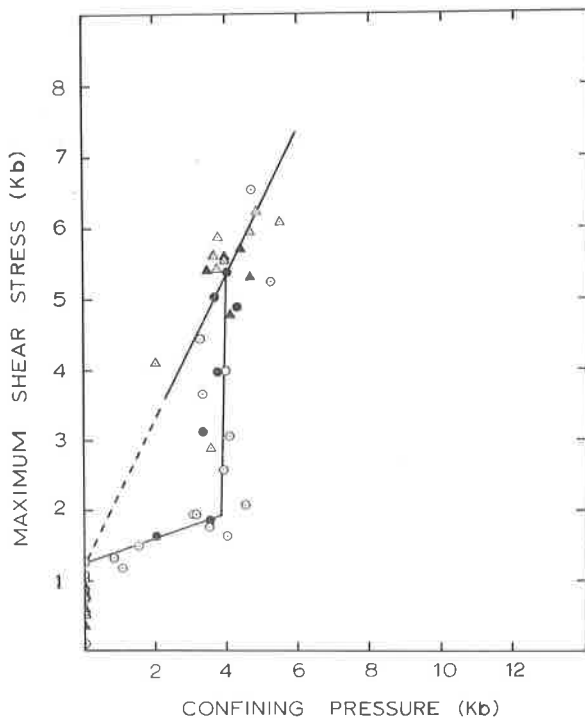
Figure 6. Maximum shear stress versus
confining fluid pressure for all experi-
ments. Symbol designation is the same
as given for Figure 2.

stress normal to the failure surface exceeds the tractive stress and no
further sliding occurs. This experimentally observed condition is given
by

$$T_M - T_o \leqslant n \, S_m. \qquad 16.$$

At point b on the experimental diagram, the slope abruptly
changes to begin the transformation segment between the slip and brittle
modes of failure. It is interesting to observe that this point also speci-
fies the state where the total strength of the material, modified by its
frictional constant, equals the value of its basic cohesive strength.
This condition is given by

$$n \, (S_m + T_o) = T_o. \qquad 17.$$

This point also coincides with the initiation of pore collapse and seems
to suggest that some sort of bulk rebonding comes into play here which
leads to a material essentially free of space defects and exhibiting the
brittle failure observed at higher stresses.

135

INTERPRETATION OF THE GRANODIORITE FAILURE DIAGRAM

IN RELATIONSHIP TO TERRESTIAL SEISMIC ACTIVITY

A review of the failure diagram as determined thus far, with the mean confining stress considered in terms of equivalent terrestial depth, shows some interesting correlations with the seismic character-istics of the earth. We have seen that granodiorite undergoes a failure transformation from a relatively quiet slip shear to a brittle one between a mean confining stress of 4.7 and 7.9 kilobars. Using the approxima-tion that 1 kilobar = 3.7 kilometers of depth for this range, these limits of mean confining stress correspond to the depth range of about 17 to 29 kilometers. According to Howell (1959), the greatest number of earth-quakes originate at a focal depth of 25 kilometers. Gutenberg (1951) has calculated the average depth of focus of shallow earthquakes at 18 kilometers, and Jeffreys (1952) gives a value of 35 kilometers. These two depths correspond to the S_m limits of the transitional segment b-e of the failure diagram, plus extension into the brittle failure region (Figure 5). Howell's average value of 25 kilometers corresponds close-ly to the midpoint of this transitional span.

Benioff (1949, 1955) has calculated strain rebound energies for successive earthquakes at a number of seismically active regions, both of shallow, intermediate and deep focal depth. All show a pattern of energy release similar in form to the rock failure diagram; that is a series of shocks of large magnitude which may be analogous to brittle failure, followed by a series of relatively low magnitude quakes similar to relatively quiet slip failure, then quakes of intermediate magnitude equivalent to the transition back to brittle failure, followed again by a series of quakes of large magnitude paralleling the reoccurrence of brittle failure. An especially clear comparison of the similarity is given in Figure 7 which is based on Benioff's data for South American deep earthquakes (Benioff, 1949). The persistent nature of this se-quential behavior is illustrated by Figure 8 which is based on Benioff's data for shallow South American earthquakes (Benioff, 1949). The con-secutive earthquakes at given seismic faults are periodic with time. Similarly, the failure diagram is constructed as a function of increas-ing time period of stress application for consecutive failures.

The failure data discussed thus far represent the limit which was obtainable with the experimental apparatus on hand. Some addi-tional data on the same granodiorite has been obtained by Riecker (1966) for the mean confining stress range of about 40 to 60 kilobars:

T_M	S_m
11.8 kb	39.8 kb
12.6	49.7
13.5	59.3

The two sets of data are combined in Figure 9. The intersection at S_m = 15 kb was established by extrapolating the earlier data upward and
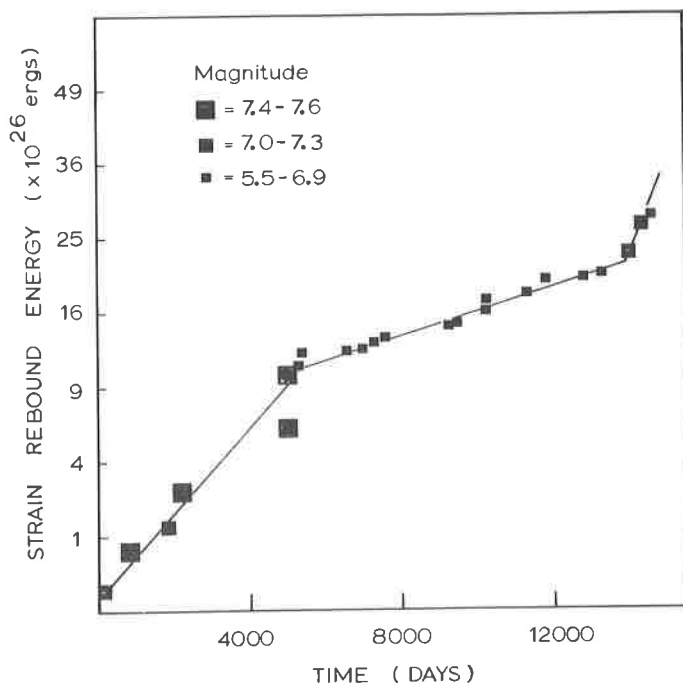
Figure 7. A plot of seismic strain rebound energy for consecutive earthquakes as a function of time from data by Benioff (1949) for South American deep earthquakes. Note the qualitative correspondence in the magnitudes and distribution of energy released with the rock failure model. The initial segment of the earthquake data appears to correspond to the region of brittle failure associated with a large instantaneous energy release. The second segment is comparable to the region of relatively quiet slip failure where the energy release is less drastic. The third segment of the earthquake data appears to correspond to the beginning of the transitional segment of the failure curve which leads back to brittle failure.

Riecker's downward. Riecker's data fits the equation,
$$T_M = 8.4 + 0.08 S_m \qquad\qquad 18.$$
with the inferred limit being $15 \leqslant S_m \leqslant ?$ kb.

Riecker's data was obtained with a Bridgman anvil type of shearing apparatus (Bridgman, 1937), and some question exists as to whether the measured stress environments in the two types of equipment are comparable. Bridgman's extensive work with anvil and hydrostatic devices (Bridgman, 1964), as well as the writer's limited experience,

137
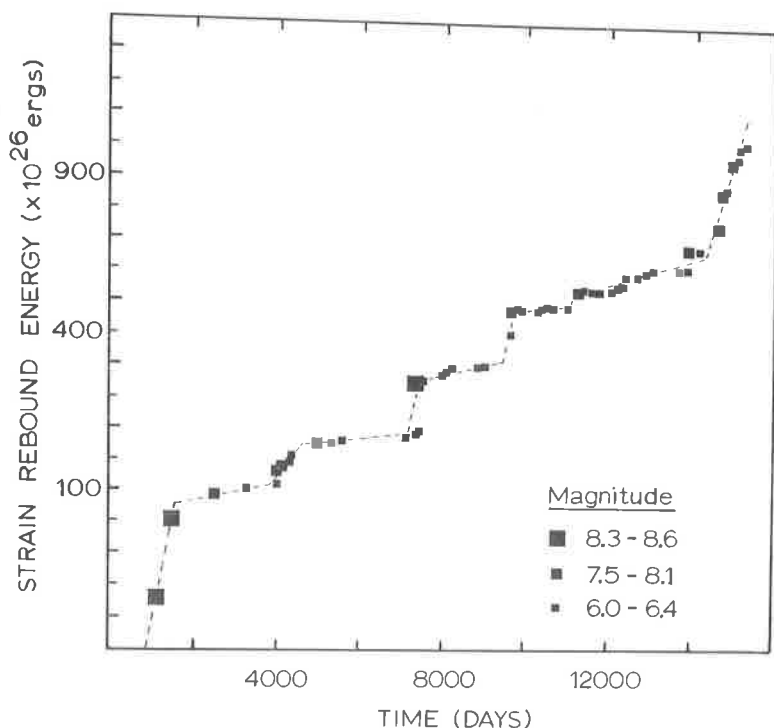
Figure 8. A plot of the seismic strain rebound energy for consecutive shallow South American earthquakes (Benioff, 1949). The alternating pattern of greater and lesser magnitude quakes with time persists and seems to be a general pattern of behavior.

suggests that in this pressure range data from the two types of equipment should agree to within 10 or 15 percent. This is within the range of error of triaxial test data.

Some idea of the validity of Riecker's data can be obtained by comparing his shear strength values with those determined by dynamic means. For example, at 50 kb of confining pressure, Cherry (1966), using the Hugoniot elastic limit, obtained a maximum shear strength of 14.8 kilobars. This is in reasonable agreement with Riecker's 12.6 kb.

Support for the compatibility of the two sets of data can be found in the correlation which exists in the abrupt change in slope of the failure curve at S_m = 15 kilobars (Figure 9) indicating a change in the mode of failure from brittle shear to some other, and the appreciable change in physical characteristics of granodiorite observed at an estimated peak shock stress of about 15 kb during detonation of the 5.0 ± 1.0 kiloton Hardhat nuclear device (Short, 1966). A graphical representation

138
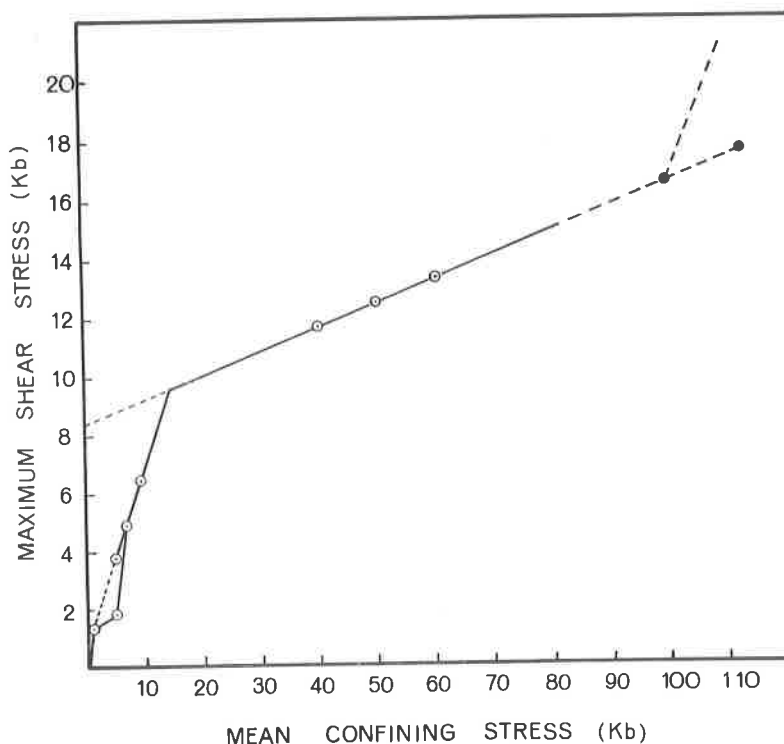
Figure 9. The extended failure diagram resulting from the combination of the experimental data of this study with that of Riecker (1966) at a higher stress level. Darkened circles are calculated points.

of the sudden decrease in Young's modulus reported by Short (1966) is given in Figure 10 to illustrate this point. The available evidence seems adequate to justify combining the two sets of data.

The apparent upper limit for brittle failure at S_m = 15 kb corresponds to a terrestial depth of about 55 kilometers and is in reasonable agreement with both the greatest depth of the Mohorovičić discontinuity beneath mountain ranges and the lower boundary for shallow earthquakes.

The linearity and very shallow but positive slope of the Riecker segment of the failure curve beyond S_m = 15 kb suggests the possible reoccurrence of a slip mode of shear failure. The very low coefficient of internal friction for this region of failure (n = 0.08) correlates nicely with the so-called "plastic zone" of the earth's interior beginning at a depth of about 55 kilometers (Anderson, 1962). It is interesting to note that according to the failure diagram rock is in an elastic state beneath the failure curve, at least for short periods relative to geologic time, and it is well known that in the so-called "plastic zone" shear waves are supported and earthquakes do occur.

139
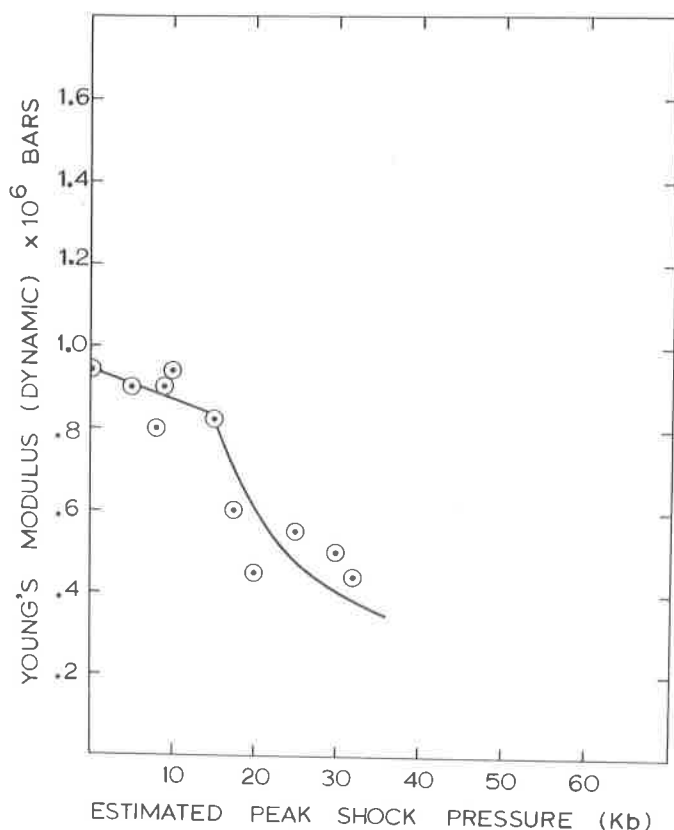
Figure 10. A representation of the Young's modu-
lus data given by Short (1966) for granodiorite
stressed by the Hardhat 5.0 ± 1.0 kiloton nu-
clear explosion. The sharp change in Young's
modulus at about 15 kilobars appears to cor-
respond with the predicted intersection point of
the data of this work with that of Riecker, mark-
ing a transformation to a possible slip shear
mode of failure.

The failure diagram developed thus far (Figure 9) represents
the limit of experimental data. The apparent correlation with the pat-
tern of sequential earthquakes seems to persist, and if real it would
seem to suggest a cyclic increase and decrease of triaxial stress which
at a particular locality periodically exceeds the limit of stability as
specified by the failure curve. According to the curve, stress relief
need occur only in the immediate vicinity of the failure surface in a
medium which is large relative to the size of the rupture. The bulk
rock would remain stable at stress intensities below the failure curve.

EXTRAPOLATION OF THE FAILURE CURVE TO A HIGHER

STRESS LEVEL AND INTERPRETATION ACCORDING TO

EQUIVALENT TERRESTIAL DEPTH

In addition to the apparent similarity of the failure curve with the pattern of sequential earthquakes at particular seismic zones, it also seems to correlate with the depth distribution of zonal boundaries of maximum and minimum seismic activity. Foci of serious disturbances peak at depths of about 25, 400 and 600 kilometers (Howell, 1959), with diminished activity in between. With respect to the failure diagram, this seems to correlate with the alternate occurrence of brittle and quiet slip failure, respectively.

It is possible to explore the apparent correlation of the failure diagram to greater equivalent terrestial depth by mathematically constructing the end point of the Riecker segment of the curve. This can be done if the assumptions are made that this segment represents a second region of slip failure analogous to that observed at lower stresses, and that it obeys the same modified Coulomb criteria. A possible cause for the reoccurrence of slip shear is not known, but it would be expected to be more fundamental than the fracture network discussed earlier.

Since,

$$T_M = f\ (S_m,\ t), \hspace{4cm} 19.$$

where f stands for function of, and t represents temperature, differentiation of the modified Coulomb expression,

$$T_M = T_o + n\ S_m, \hspace{4cm} 20.$$

yields,

$$dT_M = n\ (t)\ (dS_m)t + S_m\ (\tfrac{dn}{dt})\ (dt)S_m, \hspace{2cm} 21.$$

where

$$n\ (t) = \left(\frac{\delta\ T_M}{\delta\ S_m} \right)_t, \hspace{3cm} 22.$$

and

$$S_m\ \frac{dn}{dt} = \left(\frac{\delta\ T_M}{\delta\ t} \right)_{S_m}. \hspace{3cm} 23.$$

The above holds true providing that T_o is a true constant and independent of temperature.

From equation 23,

$$\Delta\ T_M \simeq S_m\ \Delta\ n. \hspace{4cm} 24.$$

Taking S_m = 15 kilobars, and Δn = (0.59 - 0.08) = 0.51, then ΔT_M = 7.7 kb. Since initially T_M = 9.7 kb, the terminal value must be 7.7 + 9.7 = 17.4 kb. Applying this value to the modified Coulomb equation,

$$T_M = 8.4 + 0.08\ S_m, \hspace{4cm} 25.$$

yields $S_m = 112$ kilobars. The limits of the Riecker segment, therefore, are $15 \leqslant S_m \leqslant 112$ kb. Using the approximation, 1 kb $\simeq 3.5$ km for this level of equivalent terrestial depth, the end point of the Riecker segment is equivalent to approximately 390 kilometers of depth.

If the Riecker segment does indeed represent a reoccurrence of a slip shear failure, then we also may assume that its frictional behavior will be similar to that experimentally observed between the lower stress range $S_m = 0.74$ to 5.8 kb. A transformation to a new mode of failure might be expected, therefore, when

$$n (S_m + T_o) = T_o. \qquad\qquad 26.$$

The known values of $n = 0.08$ and $T_o = 8.4$ kb yield $S_m \simeq 97$ kb. This value of mean confining stress is equivalent to an approximate terrestial depth of 340 kilometers. The inner boundary of the earth's outer "plastic zone" and the outer boundary of the second zone of peak seismic activity are at about this depth.

The renewed zone of seismic activity begins at about 350 km and peaks at about 400 km (Howell, 1959). Again, if the analogy between brittle failure and high magnitude quakes is real, and if the Riecker segment does in fact represent the reoccurrence of a slip shear, then the constructed transformation point at about 97 kb (about 340 km) and end point at about 112 kb (about 390 km) would appear to be valid, and a transformation back to a brittle mode of failure at higher stress levels would seem to be indicated. The peak in seismic activity at about 400 km would correspond to the upper limit of the transition span, and this is similar to the situation observed with the transition at lower stress.

It seems, therefore, that not only does the failure diagram apparently correlate with the sequential pattern of earthquakes at any particular depth in the earth, but also with the distribution pattern of alternating zones of maximum and minimum seismic activity with depth.

There is no experimental basis for further speculation. However, the existence of an additional peak of renewed seismic activity at about 600 kilometers and an abrupt absence of seismic disturbance beyond about 700 kilometers suggests that it may represent the end point of the speculated "upper brittle zone" and transition to a state approaching plasticity on a regular rather than geologic time scale. Extrapolation of the decreasing coefficient of friction for consecutive zones of slip failure with increasing stress indicates that if a third zone of slip-type failure were to occur beyond 650 kilometers, the frictional coefficient would be close to zero.

Since the triaxial experiments upon which the failure diagram is based were performed at room temperature, the effect of increasing temperature on the strength of the rock due to the geothermal gradient must be considered.

High pressure experimentation has shown that the melting temperature of silicates and oxides increase with pressure (Hall, 1958, and Barth, 1962). The changes show agreement with the assumed

geothermal gradient. In addition, diamond synthesis experiments have shown that the rigidity of rock material remains high at elevated temperatures and pressures. The main problem in growing large crystals is the persistent vicinal pressure drop due to the volume decrease when graphitic carbon goes to diamond. Although heated from about 1100 to 1500°C, the surrounding material fails to comply with the volume change. As a result the pressure drops and growth stops. Qualitatively, therefore, the increase in temperature with depth may be compensated for to some extent by an increase in the refractoriness of the rock. This, plus the current concept of crustal rock down-dragging at seismically active regions (Isacks et al, 1968), might explain the apparent correlation between the laboratory rock failure data and the pattern of seismic disturbances.

One further correlation is possible between the nature of sequential earthquakes and behavior predicted by the failure diagram. An apparent correlation can be shown between the calculated seismic energy released by earthquakes, and by hypothetical subsurface rupturing and faulting according to the failure model. The correctness of the respective mathematical derivations used for the calculations is open to some doubt, but the two sets of results do show a reasonable agreement.

The seismic wave energies for sequential earthquakes such as shown in Figures 7 and 8 have been calculated by Benioff (1949) according to the following derivation: The potential energy of a volume, V, of material having a shear constant, G, and an average strain, S, immediately prior to an earthquake, is given by

$$E_p = \frac{G V S^2}{2}. \qquad 27.$$

The energy released in the form of seismic waves is given by

$$E_s = f \left(\frac{G V S^2}{2} \right), \qquad 28.$$

where f is the fraction of the potential energy released as seismic waves. If it is assumed that the strain at the earthquake fault is reduced to zero as a result of displacement along the fault, then

$$S = c d, \qquad 29.$$

where d is the displacement along the fault and c is a proportionality constant. The seismic energy, therefore, is equal to

$$E_s = \frac{f G V c^2 d^2}{2}, \qquad 30.$$

and setting

$$\frac{(f G V c^2)^{1/2}}{2} = C, \qquad 31.$$

we have

$$E_s = C^2 d^2. \qquad 32.$$

The displacement at the fault, therefore, is proportional to the square root of the seismic wave energy.

By applying the above equation to one derived earlier by Guten-
berg and Richter (1942, 1949) which relates the seismic energy of
earthquakes to their magnitude,

$$\log E_s = K_1 + K_2 M, \qquad 33.$$

where K_1 and K_2 are constants which depend on the means used to
determine the magnitude, M, we have

$$\log (E_s)^{1/2} = \log C d = K_1 + K_2 M, \qquad 34.$$

Rearrangement of terms gives the following relationship between the
constant C, magnitude, and fault displacement,

$$C = \frac{10^{K_1 + K_2 M}}{d}. \qquad 35.$$

The accuracy of the above equations is not known with certainty, but it
is generally believed they yield at least a large fraction of the energy
released in the form of seismic waves.

The derivation used to calculate hypothetical strain release
energy for subsurface rupturing according to the rock failure model is
based on the mathematical solution by Starr (1928) for shearing rupture
in an isotropic solid. In his model, Starr considers the creation of a
long thin fault with dimensions small compared to subsurface depth.
Application of Starr's equations to the terrestial depth range covered
by the present failure model (Figure 9) does not permit observance of
the depth restriction if a fault size comparable to those associated with
real earthquakes is to be considered.

Orowan (1960) has interpreted Starr's equations in the following
form,

$$E = \frac{\pi}{4} (1 - 2u) \frac{L h^2}{G} T_M^2 \qquad 36.$$

where E is the difference in elastic energy of the body without and with
a crack, u is the Poisson ratio for the material, L is the length of the
crack and h is its height. G is the bulk shear modulus, and T_M is the
shearing stress required to produce the fracture.

The areal displacement of the crack normal to its length is
given by

$$A = 2 c (T_B - T_A), \qquad 37.$$

where c is a constant for the material under consideration (granodio-
rite), T_B is the initial shear stress along the fault in the direction of
displacement, and T_A is the terminal shear stress.

Since the average stress during displacement is $\frac{T_B + T_A}{2}$, the
work done is

$$W = \frac{T_B + T_A}{2} 2 c (T_B - T_A) h = h c (T_B^2 - T_A^2). \quad 38.$$

The constant c for the material may be determined by setting $T_A = 0$,
and

$$c = \frac{1}{h} \frac{\pi}{4} (1 - 2u) \frac{L h^2}{G}, \qquad 39.$$

in units of cm^4/dynes. The bulk elastic constants for granodiorite are

available to about 50 kilobars and are given in Table 1.

The energy converted to frictional heat during displacement is given by

$$H = 2 h c (T_B - T_A) T_A, \qquad 40.$$

where T_A is the shear stress where sliding stops.

The net strain release energy available for seismic wave generation is equal to

$$E_s = (W - H) = h c (T_B - T_A)^2, \qquad 41.$$

or

$$E_s = \frac{\pi}{4} \frac{(1 - 2u)}{G} L \, \Delta T^2 h^2, \qquad 42.$$

which bears a resemblance in form to equation 30. Since equation 30 would be expected to yield no more than a large fraction of the seismic energy released by an earthquake, equation 42 should yield a comparatively higher value for E_s, providing, of course, both the assumptions of its derivation and its application to the failure model are valid.

Calculated values of W, H, and (W - H) for selected values of T_M from the granodiorite failure curve are given in Table 1. Elastic constant data used in the calculations are given in Table 2. The magnitudes for the calculated energies are a function of the dimensions chosen for the hypothetical failure surface. For want of better knowledge, a 50 by 10 kilometer fault was arbitrarily selected. This is the size used by Orowan (1960) in his discussion on the mechanism of seismic faulting, and is based on Jeffreys (1952) interpretation of the usual time period of seismic pulses from deep earthquakes. A dimensional discrepancy of $\pm$ 50 percent would not seriously affect the overall magnitude of the calculated energies.

The range of seismic wave energies determined by Benioff (1955) for shallow earthquakes at Tonga-Kermadec is to approximately 10^{25} ergs, and to about 10^{28} ergs for successive earthquakes at intermediate depth. Values for shallow, intermediate and deep South American earthquakes (Benioff, 1949) range to about 10^{29}, 10^{28} and 10^{27} ergs, respectively. Each of the above localities show the same general stepwise distribution of energy with time as illustrated in Figures 7 and 8. According to Gutenberg (1956) the energy released from a single earthquake of high magnitude and deep origin is of the order of 10^{22} ergs.

The equivalent strain release energy calculated for hypothetical subsurface rupturing of Hardhat granodiorite according to the failure model ranges from about 10^{24} to 10^{27} ergs. Tabulated data for various ranges of maximum shear stress and mean confining stress (depth) are given in Table 1. The agreement appears to be reasonable, but with the uncertainties involved, this may be fortuitous.

What is needed now are additional experimental data for other types of normally brittle igneous rock, and to higher stresses. If it should be established that the failure curve shown for granodiorite has a general validity for normally imperfect igneous rock, then the model

145

Table 1. Calculated Work (W), Heat (H), and Potential Seismic Wave (W - H) Energies for a Hypothetical Subsurface Rupturing of Hardhat Granodiorite for Various Ranges of Maximum Shear Stress According to the Failure Diagram.

T_B	S_m	T_A	S_m	c	W	H	(W–H)
1.82 kb	4.7 kb	1.15 kb	0.74 kb	5.8 $\frac{cm^4}{dyne}$	1.15×10^{25} ergs	0.89×10^{25} ergs	2.6×10^{24} ergs
5.48	7.9	1.82	4.7	5.8	15.4×10^{25}	7.7×10^{25}	7.7×10^{25}
9.71	15	5.48	7.9	5.8	3.7×10^{26}	2.7×10^{26}	1.0×10^{26}
16.?	97	9.71	15	5.8	9.8×10^{26}	7.4×10^{26}	2.4×10^{26}
17.4	11?	9.71	15	5.8	12.1×10^{26}	8.7×10^{26}	3.4×10^{26}
17.4	11?	1.15	0.74	5.8	1.7×10^{27}	0.2×10^{27}	1.5×10^{27}

Table 2. Approximate Bulk Elastic Constants for Hardhat Granodiorite

	at 1 bar	5 kb	10 kb	20 kb	40 kb
K (x 10^{12} dynes cm^{-2})	0.55	0.56	0.57	0.60	0.66
E (x 10^{12} dynes cm^{-2})	0.95	0.9	0.85	0.6	0.6
G (x 10^{12} dynes cm^{-2})	0.37	0.36	0.34	0.23	0.22
u (Poisson ratio)	0.23	0.23	0.25	0.33	0.35

Values for the bulk compression modulus are from data by Stephens (1964).

Values for Young's modulus are approximated from dynamic data given by Short (1966).

may contribute to the understanding of the nature of seismic disturbances.

REFERENCES CITED

Anderson, Don L., 1962, The plastic layer of the earth's mantle: Sci. Am., v. 207, p. 52.

Barth, F. W., 1962, Theoretical petrology: 2nd Ed., John Wiley & Sons, Inc., p. 134.

Benioff, H., 1949, Seismic evidence for the fault origin of ocean deeps: Bull. Geol. Soc. Am., v. 60, p. 1837.

_____, 1955, Seismic evidence for crustal structure and tectonic activity: Geol. Soc. Am. Spec. Paper 62, p. 61.

Bridgman, P. W., 1937, Shearing phenomena at high pressures,

particularly in inorganic compounds: Proc. Am. Acad. Arts Sci., v. 72, p. 387.

Bridgman, P. W., 1964, Collected experimental papers of P. W. Bridgman: Harvard University Press, Cambridge, Mass., 7 vols.

Cherry, J. T., 1966, Computer calculations of explosion produced craters: Intern. J. Rock Mech. Mineral Sci., v. 4, p. 1.

Coulomb, M., 1776, Sur une application des regles maximis et minimas a quelque problemes de statique, relatif a l'architecture: Acad. Sci. Paris, Math. Phys. Mem., v. 7, p. 343.

Giardini, A. A., Lakner, J. F., Stephens, D. R., Stromberg, H. D., 1968, Triaxial compression data on nuclear explosion shocked, mechanically shocked and normal granodiorite from the Nevada test site: J. Geophys. Res., v. 73, p. 1305.

Goranson, R. W., 1940, Physics of stressed solids: J. Chem. Phys., v. 8, p. 329.

Gutenberg, B., 1951, Crustal layers of the continents and oceans: Geol. Soc. Am., v. 62, p. 427.

_____, 1956, The energy of earthquakes: Geol. Soc. London Quaterly J., v. 112, p. 1.

Gutenberg, B. and Richter, C. F., 1942, Earthquake magnitude, intensity, energy and acceleration: Bull. Seis. Soc. Am., v. 32, p. 163.

_____, 1949, Seismicity of the Earth and associated phenomena: Princeton University Press, Princeton, N. J.

Hall, H. T., 1958, Chemistry at high temperature and high pressure: Proc. Symp. on High Temp., Stanford Res. Inst., Menlo Park, Calif., p. 161.

Handin, J. R., Hager, R. V. Jr., Friedman, M., and Feather, J. N., 1963, Experimental deformation of sedimentary rocks under confining pressure: pore pressure tests: Bull. Am. Assoc. Petrol. Geol., v. 47, p. 717.

Hodgson, J. H., 1964, Earthquakes and Earth structure: Prentice-Hall, Inc., Englewood Cliffs, N. J., p. 6 and 110.

Howell, B. F. Jr., 1959, Introduction to geophysics: McGraw-Hill Book Co., New York, p. 86.

Isacks, B., Oliver, J., and Sykes, L. R., 1968, Seismology and the new global tectonics: J. Geophys. Res., v. 73, p. 5855.

Jeffreys, H., 1952, The Earth: 3rd Ed. Cambridge University Press, p. 71 and 341.

Mohr, O., 1882, Ueber die darstellung des spannungszustandes eines korperelements: Civilingenieure, v. 28, p. 113.

_____, 1900, Welche umstande bedingen die elastizitätsgrenze und den bruch eines materiale?: Zeit. Ver. Deutsch. Ingenieure, v. 44, p. 1524.

Orowan, E., 1960, Mechanism of seismic faulting: Geol. Soc. Am. Mem. 79, p. 323.

Riecker, R. E., 1966, Shear deformation of Nevada test site rock

samples to 60 kb and 1000°C.: 2nd Quart. Report (April), A. F. W. Lab., Kirkland Air Force Base, New Mexico.

Stephens, D. R., 1964, The hydrostatic compression of eight rocks: J. Geophys. Res., v. 69, p. 2967.

Stephens, D. R. and Lilley, E. M., 1966, Static PV curves of cracked and consolidated earth materials to 40 kilobars: UCRL Report No. 14711 (March), Univ. of Calif. Radiation Laboratory.

Short, N. M., 1966, Effects of shock pressure from a nuclear explosion on mechanical and optical properties of granodiorite: J. Geophys. Res., v. 71, p. 1195.

Starr, A. T., 1928, Slip in a crystal and rupture in a solid due to shear: Proc. Cambr. Phil. Soc., v. 24, p. 489.

Walsh, J. G., 1965, The effects of cracks on the compressibility of rocks: J. Geophys. Res., v. 70, p. 381.

POLLEN ANALYSIS OF AN ORGANIC CLAY FROM THE

INTERGLACIAL FLANNER BEACH FORMATION,

CRAVEN COUNTY, NORTH CAROLINA

By

Donald R. Whitehead and J. Terrance Davis
Department of Botany
Indiana University

ABSTRACT

An exposure of interglacial sediments at Flanner Beach, Craven County, North Carolina contains peaty clay with cypress stumps rooted on its surface. A brackish water facies of the Flanner Beach Formation overlies the clay disconformably. Pollen analysis of the organic clay indicates deposition in a fresh water environment. The pollen spectra suggest the existence of vegetation quite similar to the present. An interglacial correlation is thus supported. There is some indication of a slight lowering of sea level and/or deterioration of climate towards the end of the depositional interval. The pollen spectra are similar to those described previously from the interglacial Horry Clay from Myrtle Beach, South Carolina. This corroborates stratigraphic and paleontologic studies which have indicated the similarity of the two sections. It thus seems that the two organic clays date from the same interglacial, presumably the Sangamon.

INTRODUCTION

The lower Coastal Plain of the Carolinas presents a fertile field for the study of Pleistocene events in unglaciated regions. The surface formations of the region are virtually all Quaternary and recent studies have demonstrated that numerous sedimentary environments are represented as well as many different time segments of the Pleistocene (i. e., several of the interglacials and most of the Pleistocene since the Sangamon). Careful geomorphological and paleontological studies in portions of the Virginia, North Carolina and South Carolina Coastal Plain have led to an increased understanding of geomorphic history, depositional environments and Pleistocene climates (e. g., Oaks and Coch, 1963, Du Bar and Solliday, 1963; Du Bar and Chaplin, 1963; Johnson and Du Bar, 1964; Thom, 1965; Fallaw and Wheeler, 1969).

The application of pollen analysis to organic sediments has resulted in new concepts concerning the nature of Pleistocene vegetational and climatic changes. In particular, the sequence of changes since mid-Wisconsin time have been determined in southeastern North Carolina and southeastern Virginia (Frey, 1951, 1953, 1955; Harrison et al., 1965; Whitehead, 1963, 1964, 1965, 1967; Whitehead and Doyle, 1967).

Many spatial and temporal gaps remain to be filled. The available palynological data came from two circumscribed regions. Little is known concerning terrestrial environmental changes prior to mid-Wisconsin time. Although geomorphological and paleontological studies have provided considerable information on the nature of marine environments during several interglacial transgressive-regressive cycles, virtually nothing is known concerning terrestrial conditions.

Comparatively thick organic horizons are known from at least two well studied interglacial sections in the Carolina Coastal Plain. One such section occurs along the Intracoastal Waterway near Myrtle Beach, Horry County, South Carolina. At that site an organic clay (Horry Clay) with cypress stumps rooted on its upper surface lies beneath a fossiliferous facies of the Pamlico Formation (Cooke, 1937). The evidence indicates that the Pamlico Formation is marine and was deposited in fairly shallow warm water (Cooke, 1937; Du Bar and Chaplin, 1963). The Horry Clay was apparently laid down (at least initially) in fresh water. Palynological evidence suggests a vegetation and climate comparable to the present (Fray, 1952). A second virtually identical section occurs at Flanner Beach on the south bank of the Neuse River some 16 kilometers below New Bern in Craven County, North Carolina (Figure 1). The Flanner Beach section contains an organic, peaty clay with cypress stumps rooted on its surface. This is overlain by several meters of fossiliferous Flanner Beach Formation (Neuse Formation of Fallaw and Wheeler, 1969). The latter was apparently deposited in brackish to shallow marine waters (Mansfield, 1928; Du Bar and Solliday, 1963). The diatoms in the clay suggest that it was deposited in a fresh water environment with occasional influx of saline waters. Thus the two sections appear quite comparable and chronological equivalence has been suggested by several investigators (e. g., Richards, 1950).

The present paper describes the results of a study of the pollen and spores from the organic clay at Flanner Beach. The basic objectives of the study were to learn more concerning the depositional environment, to determine the nature of the vegetation and climate existing during deposition and to see if the palynological data corresponded to that derived from the Horry Clay.

Acknowledgements
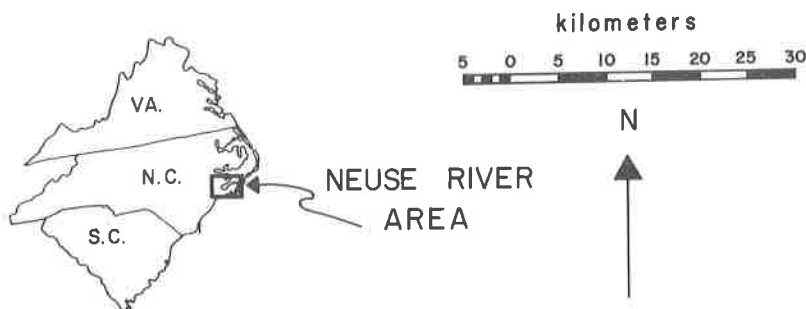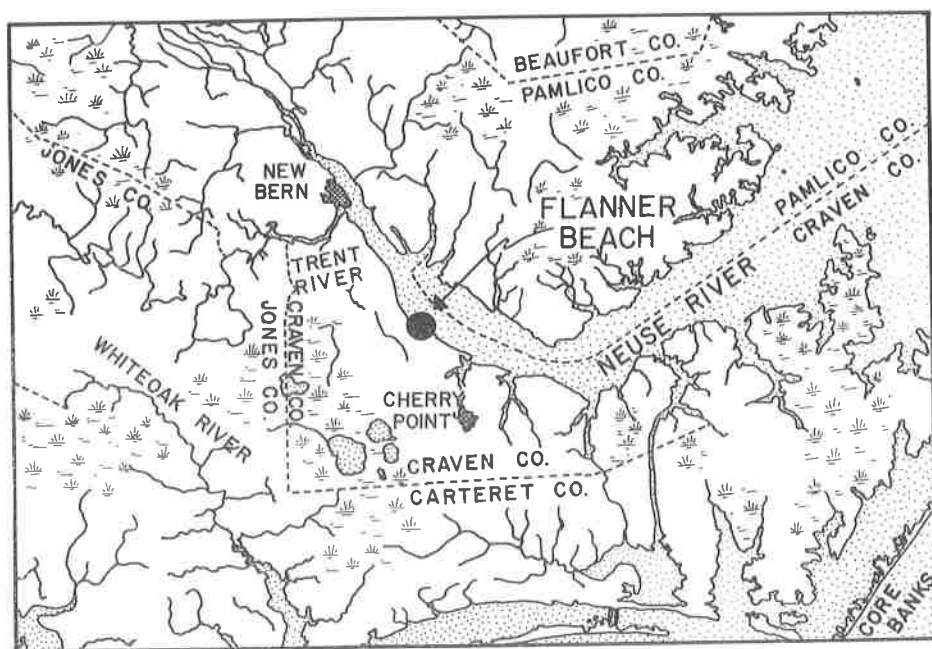
Figure 1.   Map of Flanner Beach region.

GEOLOGY OF THE AREA

An understanding of the geomorphic history of the Flanner Beach area (Figures 1 and 2) is based largely on studies of exposures along the south bank of the Neuse River below New Bern, North Carolina. Although these sections have been investigated many times (e. g., Holmes, 1885; Berry, 1926; Mansfield, 1928; Richards, 1936, 1950; Du Bar and Solliday, 1963), few detailed studies have been carried out adjacent to the river, hence the Pleistocene history remains difficult to reconstruct.

Figure 2. Photograph of site collected. Excavation at base of section is into Flanner Beach clay. Overlying sediment is fossiliferous Flanner Beach Formation.

Traditionally the land forms of the eastern half of the Coastal Plain have been interpreted as marine scarps and terrace plains resulting from interglacial high stands of the sea. At least five such formations have been recognized from the North Carolina Coastal Plain (Johnson, 1907), of which two, the youngest, appear to be represented along the Neuse below New Bern. The low-lying portion of the Coastal Plain east of Flanner Beach (with surface elevations generally below 20-25') is considered part of the Pamlico terrace, the somewhat higher land west of the site (surface elevations 30-50') is part of the Chowan terrace. The Pamlico shoreline or scarp, in places demarcated by a linear sand ridge (a barrier beach?) separates the two terrace plains.

Recent geomorphological studies of the Atlantic Coastal Plain have demonstrated that these older concepts are oversimplifications. The surficial sediments and land forms are considerably more complex, reflecting the fluctuating character of the interglacial transgressive-regressive cycles and the many sedimentary environments to be expected in a coastal region. Thus the interglacial complexes include sediments from shelf environments, beaches, barrier dunes, back-barrier lagoons and saltmarshes, estuaries, flood plains and intergradiations among these (e.g., Oaks and Coch, 1963; Johnson and

Du Bar, 1964; Du Bar and Solliday, 1963; Thom, 1965).

Recent studies of the Neuse sections near Flanner Beach have resulted in a more comprehensive picture of the Pleistocene history of that region (Du Bar and Solliday, 1963). Pliocene marine sediments occur in the vicinity of New Bern (James City Formation), but all of the overlying beds are now considered to date from a single interglacial transgressive-regressive cycle and are classified as the Flanner Beach Formation. Some of the best evidence derives from the section exposed at Flanner Beach (see Table 1) in which the lower facies appear to be transgressive, the upper regressive. At the base of the section is a carbonaceous clay, peaty at the top, with cypress stumps rooted on the surface. The nature of the sediment, the presence of cypress, and occurrence of predominantly fresh-water diatoms (but with a few marine forms) suggests deposition in a fresh-water environment (subject to some estuarine influence) during a time of rising sea level (Mansfield, 1928). The organic clay is overlain, presumably disconformably, by several meters of fossiliferous sandy clay. The molluscs and foraminifera indicate that the sandy clays were deposited in brackish embayments with evidence downstream of more open water beach environments (Du Bar and Solliday, 1963). Water temperatures somewhat higher than present seem indicated (Mansfield, 1928; Richards, 1936, 1950). The overlying sediments, sparsely fossiliferous or unfossiliferous, are considered to derive from the regressive phase of the interglacial cycle.

Thus it would appear that both fresh water and shallow marine environments are represented in the Flanner Beach Formation. A sea level higher than the present is indicated, but the extent of the transgression is not suggested. Studies of the supposedly contemporaneous Pamlico Formation in Horry County, South Carolina, suggest a sea level 10 to 40 feet higher than the present (Du Bar and Chaplain, 1963). A Sangamon age has been suggested.

PRESENT VEGETATION

The present vegetation of the Croatan area reflects the variation in topography and surficial sediments. On low clay-rich soils along the Neuse River a bottomland forest occurs. The most frequent trees in such habitats are cypress (Taxodium), gum (Nyssa), ash (Fraxinus), sweet bay (Magnolia), tulip tree (Liriodendron), willow (Salix) and cottonwood (Populus). Other trees and numerous shrubs occur as associates.

The forests of the terrace plains are quite variable. On sandier sites pines tend to predominate (both long-leaf and loblolly occur) with a variety of oaks. On soils richer in clay (the dominant soils of the region), the forest are richer and can be classified as pine and hardwoods (e. g. , Whitehead and Tan, 1967). Such forest are characterized

Table 1. Flanner Beach Section.

Description of sediment	thickness of unit	height (above MSL)
Sandy clay, gray to red-brown, much iron-staining, not fossiliferous. (equivalent to "upper regressive" and top of "basal regressive" units of Du Bar and Solliday, 1963.)	350 cm	310-660 cm.
Sandy clay, blue-gray, highly fossiliferous. (equivalent to units 2-4B, lower transgressive to basal regressive, of Du Bar and Solliday, 1963.)	200 cm	110-310 cm.

------------------------disconformity------------------------

Organic clay, blackish, peaty at top, cypress stumps rooted on surface.	at least 130 cm (base below present level of the Neuse River)	(-) 20-110 cm.

by an abundance of loblolly pine with numerous hardwood associates sweet gum (Liquidambar), dogwood (Cornus), holly (Ilex), oaks (Quercus), hickory (Carya), beech (Fagus) and maples (Acer). A variety of shrubs occur in the understory (Myrica, Clethra, Rhododendron, Rhus, Vibrunum, etc.).

FIELD AND LABORATORY TECHNIQUES

Samples were collected from a section exposed on the south bank of the Neuse River at Flanner Beach, Croatan State Forest, Craven County, North Carolina. The exposure is the same as that described and collected by Holmes (1885), Mansfield (1928) and Du Bar and Solliday (1963). The coordinates of the site are 34° 59' North Latitude, 77° 57' West Longitude. The section is described in Table 1 and illustrated in Figures 1 & 2.

A clean face was first prepared and an unsuccessful effort was made to expose the full depth of the organic clay (much of which lies below the present level of the Neuse River). Samples were taken at five centimeter intervals and were stored in sealed shell vials. A Livingstone sampler was used to core the organic clay below the base of the section.

In the laboratory samples were prepared by: (1) boiling in 10 percent KOH, (2) treating with 10 percent HCl, (3) boiling in concentrated HF, (4) acetolysing for one minute, (5) staining with basic fuschsin

and (6) mounting in silicone oil (12, 500 cs.).

Slides were counted using a Wild M11 microscope at a magnifi-
cation of 600 diameters. Difficult grains were observed with oil im-
mersion (bright field) and with phase contrast. A minimum of 300 tree
pollen was counted for each level. One pollen type, "Cupressaceae",
requires some explanation. This category includes grains of Juniperus,
Chamaecyparis and broken grains of Taxodium. Intact Taxodium grains
are relatively easy to identify because of the presence of a distinct
papillus on the grain. However, when cypress grains break open,
which is the normal situation in most sedimentary environments, a
split develops through the papillus, and the grains become indistinguish-
able from those of juniper and cedar. It is thought that the majority of
"Cupressaceae" grains actually represent broken Taxodium.

THE POLLEN DIAGRAM

The results of the study are presented in the pollen diagram
(Figure 3) and Table 2 (which includes pollen and spore types not in-
cluded on the diagram). As is evident there are few marked trends in
the diagram, hence it is difficult to differentiate zones. In general the
same pollen types occur throughout the diagram and in roughly the
same proportions. Tree types dominate the diagram, with pine,
"Cupressaceae"-Taxodium and oak the most common types. Hickory,
ash, sweet gum, ironwood, elm, birch, hazel and beech are less com-
mon but represented more or less continuously. A number of other
tree types occur occasionally in the section. Shrub types are infre-
quent, with button-bush (Cephalanthus) the only relatively common
taxon. Herbs are fairly common, with grasses, sedges, chenopods and
composites the most frequent.

A rough tripartite zonation can be made on the basis of the ap-
parent reciprocal behavior of the pine and "Cupressaceae" curves.
"Cupressaceae" grains are more abundant at the base and at the top of
the profile, pine pollen in the middle. Thus the lower 30 cm of the or-
ganic clay can be differentiated as a "Cupressaceae-herb pollen zone",
the middle 65 cm as a "pine pollen zone" and the upper 35 cm as a
"Cupressaceae-mesophyte pollen zone".

The lowest zone is characterized by a maximum of "Cupres-
saceae" pollen and maxima of grasses, sedges, composites and cheno-
pods. The mid-zone can be distinguished by the maximum of pine and
minimum for "Cupressaceae". Pollen of several aquatics is more com-
mon in this zone. The upper zone is characterized by a maximum of
Cupressaceae (and pine minimum) and by the more frequent occurrence
of grains of several mesophtic species (e. g., Nyssa, Fagus, Acer
saccharum, Picea). Colonies of the green alga, Pediastrum occur at
the top of the section and "hystrichosphaerids" are relatively common.

155

Figure 3. Pollen diagram from Flanner Beach section.

156

Table 2. Microfossils Not Included on Pollen Diagram.

Depth (cm.)	Acer rubrum	Celtis	Symplocos	Tilia	Platunus	Liriodendron	Juglans	Populus	Clethra	Ericaceae	Cyrilla
0	0.39	--	--	--	--	--	--	--	--	0.39	--
5	--	--	--	--	--	--	--	--	--	--	0.34
10	0.22	--	0.22	--	--	--	--	--	--	--	--
15	0.23	--	--	--	--	--	--	--	--	--	--
20	--	--	--	--	--	--	--	--	--	--	--
25	0.17	--	--	--	--	--	--	--	--	0.23	--
30	0.69	--	--	0.23	--	--	--	--	--	--	--
35	0.55	--	--	--	--	--	--	--	--	--	--
40	--	--	--	--	--	--	--	--	--	--	--
45	0.20	--	--	--	0.25	--	--	--	--	--	--
50	0.25	--	--	--	0.23	--	--	--	--	--	--
55	--	--	--	--	--	--	--	--	--	--	--
60	--	0.18	--	--	--	--	--	--	--	--	--
65	0.30	--	--	--	--	--	--	--	--	--	--
70	--	--	--	--	--	--	--	--	--	--	--
75	--	--	--	--	--	0.60	--	--	--	--	--
80	--	0.30	--	--	--	--	--	--	0.30	--	--
85	--	--	--	--	--	--	--	--	--	--	--
90	--	--	--	--	--	--	--	--	--	--	--
95	--	--	--	--	--	--	--	--	--	--	--
100	0.18	--	--	--	--	--	--	--	--	--	--
105	0.30	--	--	--	--	0.30	--	--	--	--	--
110	--	--	--	--	0.31	--	--	--	--	--	--
115	0.33	--	--	--	0.33	--	--	--	--	--	--
120	0.25	--	--	--	0.25	--	--	--	--	--	--
125	--	--	--	--	0.29	--	0.31	--	--	--	--
130	--	--	--	--	--	--	--	--	--	--	--
135	--	--	--	--	--	--	--	0.31	--	--	--

157

Table 2. Continued.

Depth (cm.)	Itea	Vitis	Viburnum	Sambucus	Onagraceae	Plantago	Thalictrum	Polypodium	Osmunda regalis	Osmunda cinnamomea
0	---	---	---	---	---	---	---	1.19	---	---
5	---	---	---	---	---	---	---	2.09	---	---
10	---	---	---	---	---	---	---	0.22	0.22	---
15	0.23	---	---	---	0.23	---	---	0.23	---	0.23
20	---	---	---	---	0.24	---	---	---	0.49	---
25	---	---	---	---	---	---	---	0.34	---	0.17
30	0.23	---	---	---	0.23	---	---	---	---	0.23
35	---	---	---	---	---	---	---	---	---	0.27
40	---	---	---	---	0.19	---	---	---	---	---
45	---	---	---	---	---	---	---	---	0.20	---
50	---	---	---	---	---	---	---	---	---	---
55	---	---	---	---	---	---	---	---	---	---
60	---	---	---	---	---	---	---	---	---	---
65	---	---	---	---	---	---	---	---	---	---
70	---	---	---	---	0.29	---	---	---	0.29	---
75	---	---	---	---	---	0.32	---	---	---	---
80	---	---	---	---	---	---	---	---	---	---
85	---	---	---	---	---	---	---	---	---	0.16
90	---	---	---	---	---	---	---	0.32	0.21	---
95	---	---	---	---	---	---	---	---	---	---
100	---	---	---	---	---	---	0.18	---	0.18	---
105	---	---	---	---	---	---	---	0.60	---	---
110	---	---	---	---	---	---	---	---	---	---
115	---	---	---	---	0.33	---	---	---	0.33	---
120	---	0.25	---	---	---	---	0.25	---	---	---
125	---	---	0.29	---	---	0.29	---	---	---	---
130	---	---	---	---	---	---	---	---	---	---
135	---	---	---	0.63	---	---	---	---	---	---

158

Table 2. Continued.

Depth (cm.)	Pteridium	Lycopodium inundatum	Sphagnum	Proserpinaca	Typha angustifolia	Nuphar	Nymphaea	Pontederia
0	--	--	1.59	0.39	--	--	--	--
5	--	--	--	0.34	--	--	--	--
10	--	--	0.22	--	--	--	--	--
15	--	--	--	--	--	0.23	--	--
20	--	--	0.24	--	--	0.24	0.24	--
25	0.17	--	--	--	--	--	--	--
30	--	--	--	--	--	--	--	--
35	--	--	0.27	--	--	--	--	--
40	--	--	--	--	--	0.19	--	--
45	--	--	--	--	--	--	--	--
50	--	--	0.23	--	--	--	--	--
55	--	--	0.36	--	--	--	--	--
60	--	--	--	--	--	--	--	--
65	--	--	--	--	--	--	--	--
70	--	0.88	--	--	--	--	--	--
75	--	--	--	--	--	--	--	--
80	--	--	--	0.30	--	--	--	--
85	--	--	0.50	--	--	--	--	--
90	--	--	--	--	--	--	--	--
95	--	--	0.32	--	--	--	--	--
100	--	--	0.72	0.18	--	--	--	--
105	--	--	0.30	--	--	--	--	--
110	--	--	--	0.31	--	--	--	--
115	--	--	--	--	0.66	--	--	--
120	--	--	--	--	--	--	--	--
125	--	--	--	--	--	--	--	--
130	--	--	--	--	--	--	--	--
135	--	--	--	--	--	--	--	0.31

159

INTERPRETATIONS

As mentioned previously, there are no dramatic changes in the pollen diagram. In general the same taxa are represented throughout and in roughly the same proportions. The few changes (which permitted the rough tripartite division) may not reflect major environmental alterations, but possibly local vegetational changes controlled by sea level. For example, the most obvious change in the diagram is the reciprocal fluctuation of "cupressaceae" (cypress) and pine. The changes in cypress pollen frequency could easily indicate changes in the density of cypress stands growing along the shores of the embayment, estuary or river in which the organic clays were sedimenting. Representational studies in Bladen County, North Carolina have indicated that local stands of cypress contribute significantly to the pollen rain accumulating in lakes (Whitehead and Tan, 1967). The same explanation could be forwarded for the changes in herb frequency.

Relatively temperate conditions, hence an interglacial correlation, are suggested by the pollen spectra. "Boreal" taxa (Picea and Tsuga) are represented very infrequently and only in the upper half of the profile. Virtually all entities represented by pollen are those that occur in the region at the present time. Furthermore, the pollen spectra are markedly similar to modern spectra from lakes in Bladen County. Cypress appears to be more abundant than in the Bladen samples, but otherwise the rank order and frequency of the various pollen types are similar. This would suggest that the vegetation in the Croatan area during deposition of the clays was similar to the present; hence the climate may have been comparable as well.

It is interesting that the spectra from the Flanner Beach clay are similar to those from supposed interglacial formations in the Carolinas, but quite different from those from either interstadial or stadial horizons. A very similar interglacial sequence is exposed along the Intracoastal Waterway near Myrtle Beach in Horry County, South Carolina. An organic clay (the Horry Clay) with rooted cypress stumps is overlain by a shallow water marine facies of the Pamlico Formation. The pollen spectra from the Horry Clay (Frey, 1952) are virtually identical to those from the Flanner Beach clay. Interstadial spectra are known from the Bay Lakes profiles (Frey, 1951, 1953, 1955; Whitehead, 1963, 1964, 1967) and possibly from the peats exposed along the Intracoastal Waterway near Long Beach North Carolina (Whitehead and Doyle, 1967). In the interstadial spectra, pine is much less common, and boreal elements, particularly spruce, are more frequent. The full-glacial spectra are strikingly different, in that pine is extremely abundant, boreal elements are well represented and pollen grains of temperate species are virtually absent. All of this evidence supports the interglacial corelation for the Flanner Beach clay.

Although it is evident that the regional vegetation (and climate) of the Croatan area did not change markedly during the deposition of the

organic sequence, one might suggest that a minor sea level fluctuation (and hence climatic change) took place. The evidence available suggests that the clay was deposited in a fresh water environment, with perhaps an occasional influx of saline water. The nature of the sediment, the occurrence of cypress stumps, the predominance of fresh water diatoms (Mansfield, 1928) and the presence of pollen of numerous basically fresh-water aquatics suggests this. However, the clay is significantly more organic, even peaty, at the top. In addition, there are many obvious cracks extending downward from the surface of the peaty horizon. These cracks are filled with material from the brackish water sands and clays that overlie the organic section disconformably. This might suggest a slight lowering of water level (and hence sea level) in the embayment prior to the transgression which deposited the brackish and marine facies. The pollen data corroborate this in a very general way. For example, chenopods (and cypress) are abundant at the base, fresh water aquatics are more common in the middle portion of the profile, and mesophytes (Acer saccharum, Fagus, Betula and Nyssa) and "boreal elements" (Picea and Tsuga) are more frequent in the upper half. The abundance of chenopods might indicate more pronounced brackish conditions (Suaeda and Salicornia are common salt marsh taxa). The relative abundance of fresh water aquatics could indicate a lessening of the estuarine influence. This could be due to a slight lowering of sea level, although other explanations are possible. The occurrence of boreal taxa and mesophytes in the upper half of the profile could indicate cooler (and moister?) conditions, perhaps reflecting a minor climatic fluctuation superimposed on a general interglacial trend of climatic amelioration; a trend possibly resulting in a slight lowering of sea level.

Although the evidence for a minor climatic oscillation and concordant sea level change is equivocal, it is interesting that recent geomorphological work in southeastern Virginia seems to indicate that the transgressive-regressive interglacial cycles were fluctuating in character (Oaks and Coch, 1963). Thus one might expect minor oscillations of sea level to be superimposed upon a general transgressive or regressive trend in other areas as well.

DISCUSSION AND CONCLUSIONS

The pollen data provide corroboration for previous stratigraphic studies and indicate that the organic clay from the Flanner Beach Formation is interglacial in age. The pollen spectra indicate a vegetation very similar to that presently existing on the Coastal Plain; this, in turn, would imply similar climatic conditions and the existence of edaphic situations comparable to the present.

Previous work (e. g., Mansfield, 1928) has suggested that the clay was deposited in a stream channel, perhaps in the upper reaches

of an estuary, where the environment was basically fresh water, but with occasional saline influence. The pollen evidence substantiates this. Pollen or spores of many aquatic plants are represented (Sagittaria, Typha latifolia, Typha-Sparganium, Potamogeton, Pontederia, Nuphar, Nymphaea, Myriophyllum, Polygonum Persicaria, Proserpinaca, Isoëtes). Although the majority of the species of these taxa grow in fresh water, there are species of Sagittaria, Typha, Potamogeton, Nuphar and Isoëtes that either tolerate brackish water or occur regularly in brackish environments (Muenscher, 1944). In addition, colonies of the fresh water green alga, Pediastrum, occur in the profile. Suggestion of brackish influence comes from the marine diatoms reported by Mansfield (1928) and possibly from the hystrichosphaerids occurring in the profile. Some caution is indicated in dealing with these microfossil data, as one must consider the provenance of the material. For example, it is possible that the pollen of fresh water aquatics was carried in from much further upstream. On the other hand, the marine diatoms (and hytrichosphaerids) might not derive from the clay itself.

A careful examination of the peaty surface of the clay indicated the presence of many deep cracks which were filled with sediment and shell material from the overlying brackish water facies of the Flanner Beach Formation. It is thus possible that the marine diatoms actually derived from the filling of the cracks rather than from the clay. The bulk of the evidence does point to a fresh water environment, possibly either the upper reaches of an estuarine system or an essentially non-saline embayment behind a closed barrier system.

It is interesting to compare the Flanner Beach organic horizon with the Horry Clay from South Carolina, since the two are similar and very probably date from the same interglacial. The stratigraphy of both sites is comparable, the character of the clays similar, cypress stumps occur in both sections and the pollen spectra are similar. Evidence concerning the depositional environment for the Horry Clay is a little more difficult to interpret, because the pollen data (Frey, 1952) suggests fresh water, while the diatoms (Cooke, 1937) brackish or marine. To the present writers a fresh water origin seems most likely because of the nature of the sediments, the occurrence of cypress and the presence of pollen of fresh water aquatics. One might question the derivation of the marine diatoms, as Cooke (1937) mentions that the surface of the Horry Clay is riddled with borings. These might have permitted the introduction of marine diatoms from the overlying Pamlico Formation. Despite these minor interpretational problems, it would appear that the depositional environments for the Flanner Beach clay and the Horry Clay were similar, and that the regional vegetation (and climate) existing during deposition was similar also. This in turn could be taken to indicate chronological equivalence of the two deposits.

REFERENCES

Berry, E. W., 1926, Pleistocene plants from North Carolina: U. S. Geological Survey, Prof. Paper 140-C, p. 97-117.

Cooke, C. W., 1937, The Pleistocene Horry Clay and Pamlico formation near Myrtle Beach, South Carolina: Wash. Acad. Sci. Jour., v. 27, p. 1-5.

Du Bar, J. R., and Chaplin, J. R., 1963, Paleoecology of the Pamlico Formation (late Pleistocene), Nixonville quadrangle, Horry County, South Carolina: Southeastern Geology, v. 4, no. 3, p. 127-165.

Du Bar, J. R., and Solliday, J. R., 1963, Stratigraphy of the Neogene deposits, Lower Neuse Estuary, North Carolina: Southeastern Geology, v. 4, p. 213-233.

Fallaw, W., and Wheeler, W. H., 1969, Marine fossiliferous Pleistocene deposits in Southeastern North Carolina, Southeastern Geology, v. 10, p. 35-54.

Frey, D. G., 1951, Pollen succession in the sediments of Singletary Lake, North Carolina: Ecology, v. 32, p. 518-533.

_____, 1952, Pollen analysis of the Horry Clay and a seaside peat deposit near Myrtle Beach, South Carolina: Am. Jour. Sci., v. 250, p. 212-225.

_____, 1953, Regional aspects of the late-glacial and post-glacial pollen succession of southeastern North Carolina: Ecol. Monogr., v. 23, p. 289-313.

_____, 1955, A time revision of the Pleistocene pollen chronology of southeastern North Carolina: Ecology, v. 36, p. 762-763.

Harrison, W., Malloy, R. J., Rusnak, G. A., and Terasmae, J., 1965, Possible late Pleistocene uplift Chesapeake Bay entrance: Jour. Geol., v. 73, no. 2, p. 201-229.

Holmes, J. A., 1885, Taxodium (cypress) in North Carolina Quaternary: Elisha Mitchell Sci. Soc. Jour., v. 2, p. 92-93.

Johnson, B. L., 1907, Pleistocene terracing in the North Carolina coastal plain: Science, v. 26, no. 671, p. 640-642.

Johnson, H. S., and Du Bar, J. R., 1964, Geomorphic elements of the area between the Cape Fear and Pee Dee Rivers, North and South Carolina: Southeastern Geology, v. 6, p. 37-48.

Mansfield, W. C., 1928, Notes on the Pleistocene faunas from Maryland and Virginia and Pliocene and Pleistocene faunas from North Carolina: U. S. Geol. Surv. Prof. Paper 150-C, p. 129-140.

Muenscher, W. C., 1944, Aquatic plants of the United States: Comstock Publishing Co., Ithaca, 374 p.

Oaks, R. Q., and Coch, N. K., 1963, Pleistocene sea levels, southeastern Virginia: Science, v. 140, no. 3570, p. 979-983.

Richards, H. G., 1936, Fauna of the Pleistocene Pamlico Formation of the southern Atlantic Coastal Plain: Geol. Soc. Am. Bull., v.

47, p. 1611-1656.

Richards, H. G., 1950, Geology of the Coastal Plain of North Carolina: Am. Phil. Soc. Trans., v. 40, p. 1-83.

Thom, B. G., 1965, Relationship of Carolina Bays to regional geomorphology: (Abstract) Annual Meeting, Geol. Soc. Am.

Whitehead, D. R., 1963, "Northern" elements in the Pleistocene flora of the Southeast: Ecology, v. 44, p. 403-406.

_____, 1964, Fossil pine pollen and full-glacial vegetation in southeastern North Carolina: Ecology, v. 45, p. 767-776.

_____, 1965, Palynology and Pleistocene phytogeography of unglaciated eastern North America; in Wright and Frey (eds.), The Quaternary of the United States: Princeton Univ. Press., p. 417-432.

_____, 1967, Studies of full-glacial vegetation and climate in southeastern United States; in Cushing and Wright (eds.), Quaternary paleoecology, Yale Univ. Press, p. 237-248.

Whitehead, D. R., and Doyle, M. V., 1967, Mid-Wisconsin interstadial peats near Long Beach, North Carolina: (abstract), Annual Meeting, Geol. Soc. Am., S. E. Sect.

Whitehead, D. R., and Tan, K. W., 1967, On the relationship between modern vegetation and pollen rain in Bladen County, North Carolina: unpublished manuscript.

SPATIAL VARIATION OF FLOOD FREQUENCIES

AS RELATED TO HYDRAULIC GEOMETRY

By

Richard A. Stephenson
Department of Geography
University of Georgia
Athens, Georgia

ABSTRACT

Hydraulic geometry is, in essence, the description of channel characteristics and their relationship to streamflow. This study describes six flood frequencies as they are related to six hydraulic parameters. The relationship between floods and channel characteristics has been exhibited in theory as well as numerous studies. This study shows how they are related and how the relationship varies spatially. From the results using standardized residuals from regression, a significant variation was found to exist in the sample basins which are located in the southern Blue Ridge Mountains. Also, it was found that the relationship between flood frequencies and hydraulic parameters is rather weak.

INTRODUCTION

Investigations concerning flood magnitudes remain largely empirical. Many hypotheses and generalizations still need to be presented and tested in the field, for many of the formulae now are derived from isolated studies and laboratory experiments. However, numerous quantitative studies have been accomplished in the past several decades (Benson, 1959; Wong, 1963).

Many interrelated factors affect floods and their magnitudes. Several equations have been formulated to express this multivariate relationship. Which equation expresses this relationship more appropriately is open to conjecture, for each seems to emphasize different factors and relationships that affect floods. This study, though only considering hydraulic geometry as the explaining variables, will attempt to show still another factor that affects floods. This factor is spatial variation, for it is surmised that any variation in floods is due to a variation in hydraulic geometry as well as location. It is assumed that similar hydrologic processes exist on all drainage basins. However, it is anticipated that various factors do not exist in the same

165

magnitude, but vary from basin to basin.

STUDY AREA

The general location of the study area is the extreme eastern portion of the Tennessee River drainage system. More specifically, twenty-five separate drainage basins within this network were chosen for investigation. The criteria for basin selection were: (1) 25-year length of record, (2) small size and (3) little effect of man, such as impoundments. These basins are located entirely within the Southern Blue Ridge Mountains of North Carolina, Tennessee and Georgia (Figure 1).

The drainage areas ranged in size from approximately 5.5 to 177 square miles. These basins varied not only in size, but in other characteristics as well. Of particular importance with regard to varia-- tion in basin features is the complex geology, orographic surplus and deficient precipitation zones, humid and dry slope vegetation associations and topographic expression. It is under these varied conditions that the investigation of stream behavior must operate.

THEORETICAL CONSIDERATIONS

Hydraulic geometry, in simplest terms, is the description of channel characteristics in relation to the flow of water. This relationship is indicated by the basiç equation,

$$Q = AV \qquad (1)$$

where Q indicates discharge, A is the cross-sectional area of the stream and V is velocity at a given cross-section. However, Kazmann (1965) states that this equation is deceptive due to inexact approximations of stream flow.

Leopold and Maddock (1953) found that channel characteristics differ only in numerical values of coefficients and exponents as related to discharge. The equations

$$w = aQ^b \qquad (2)$$
$$d = cQ^f \qquad (3)$$
$$v = kQ^m \qquad (4)$$
$$l = pQ^j \qquad (5)$$

where w is width, d is mean depth, v is mean velocity, l is suspended-sediment load, Q is discharge, and a, c, k, p, b, f, m and j are numerical constants. The relationship revealed by the foregoing equations is, in essence, hydraulic geometry. In addition to the previous equations, Wolman (1955) added two more relationships, as follows:

$$S = tQ^z \qquad (6)$$
$$n^1 = rQ^y \qquad (7)$$

where S is stream slope, n^1 is a roughness parameter, Q is again
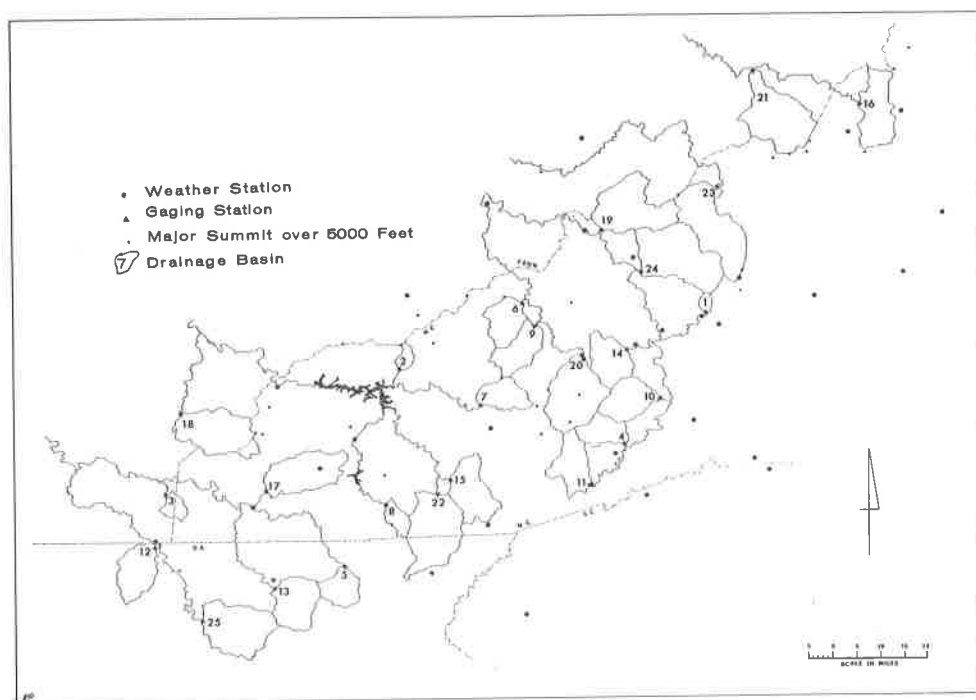
Figure 1. Location of study area.

discharge and t, r, z and y are numerical constants. From these two studies it is apparent that a relationship can be expressed between discharge and hydraulic characteristics. These numerical constants vary in different samples, however, since the coefficient is usually the a-value or Y intercept and the exponent is usually the b-value or regression slope or surface in a regression analysis.

WORKING HYPOTHESES

One would gather from the work accomplished by Leopold, Maddock, Wolman and others, that the relationship between stream discharge and channel variables has been adequately resolved. In many respects, what has been accomplished is limited due to the nature of statistical methodology. It is veritable that regression analysis is usually employed to show the functional relationship between discharge and various parameters; but the results must be qualified. The basic problem is that not all cases or observations in the relationship fall on the regression surface as set forth in the statistical model. Thus, the coefficients and exponents are only approximations of the relationship involved.

It is obvious that all cases do not fit the regression surface

except under very unusual circumstances. In fact, many cases in the sample are usually quite scattered or occur by chance. To correct skewed distributions, transformations are made. To create a seemingly more significant correlation, coefficient of determination or regression value, additional variables are entered into the model. Or, if one chooses, a simple "x is a function of y" relationship is ascertained, even when a multivariate relationship is known to exist. Thus, these problems in correlation and regression are created when sample size and parameters change. Two hypotheses can be stated from the foregoing presentation. First, that the relationship between flood frequencies and channel factors varies from one basin to another; and second, that the variation between flood frequencies and channel factors tends to change as flood magnitude increases.

DEPENDENT AND INDEPENDENT VARIABLES

The discharge variables used in this study are flood frequencies using a method adopted by the U. S. Geological Survey. The equation

$$T = N + 1 / m \qquad (8)$$

where T is recurrence interval in years, n is number of years of record, and m is the magnitude of flood with 1 being the highest. This equation ranks the annual flood as it is related to a recurrence interval for the period of record. Thus, flood frequency may be simply defined as the relationship between certain magnitudes of discharge and their respective recurrence intervals. Once the data are collected, plotting is done on special probability graph paper which was supplied by U. S. G. S. Finally, a frequency curve is plotted to obtain the flood magnitude.

The flood frequencies chosen for this study are: (1) mean annual flood or the 2.33-year flood, (2) 5-year flood, (3) 10-year flood, (4) 25-year flood, (5) 50-year flood and (6) 100-year flood. (Table 1).

The flood magnitudes for each flood frequency were measured in cubic feet per second per square mile (cfsm or cfm). The purpose for using this measurement was to adjust discharge to the drainage area. This produces a dimensionless parameter which is considered to be a more critical value than cubic feet per second (cfs).

From the theoretical framework, the independent or channel variables chosen for this study are: (1) channel gradient in feet per mile, (2) mean channel width in feet, measured from the top of the channel bank, (3) mean channel depth in feet, also measured from the top of the channel, (4) mean channel cross-sectional area in square feet, (5) channel length in miles and (6) mean channel material in cubic feet, measuring a sample of the largest material in the channel bed which is a measurement assumed to be similar to Wolman's n[1] (Table 1). These variables were sampled along the trunk stream in the study basins at selected cross-sections. It can be noted that several of these

Table 1. Flood and Channel Data.

Stream Basin	$Q_{2.33}$	Q_5	Q_{10}	Q_{25}	Q_{50}	Q_{100}
Beetree	47.99	91.58	131.87	188.64	224.36	263.74
Noland	71.01	85.14	82.25	113.41	123.91	134.06
Turtletown	25.65	31.60	35.50	43.87	49.07	54.46
Davidson	76.73	111.39	144.80	188.12	220.30	252.48
Hiawassee	47.91	76.92	102.75	136.81	169.23	210.99
Cataloochee	41.67	63.41	83.50	109.76	129.07	148.89
Scott	30.18	46.55	60.65	79.09	93.20	154.04
Nantahale	51.06	71.77	90.37	114.84	133.91	152.22
Jonathan	31.39	42.88	53.60	67.38	77.34	88.06
Mills	43.48	75.71	104.95	142.43	172.41	200.90
French Broad	64.06	107.51	147.28	199.56	239.32	278.35
Fightingtown	41.61	59.24	75.46	96.61	122.71	150.56
Nottely	52.14	70.86	88.24	110.96	128.34	145.05
Hominy	31.33	61.40	89.60	126.57	154.14	182.33
Collasaja	43.93	76.88	107.51	146.82	177.46	206.94
Watauga	101.87	202.64	291.85	408.59	498.35	584.80
Valley	50.48	87.50	121.15	166.35	199.52	234.62
Tellico	45.76	63.56	78.53	100.56	117.23	206.21
Big Laurel	32.14	53.17	71.43	96.03	114.29	132.54
Pigeon	62.03	99.25	133.46	178.20	212.41	246.24
Doe	41.97	76.64	109.49	151.82	183.21	216.06
Little Tennessee	28.00	43.93	58.57	77.86	92.14	106.43
Cane	42.36	80.57	114.97	161.78	196.82	231.85
Ivy	24.68	40.51	55.38	75.00	89.56	104.43
Toccoa	28.67	37.29	45.20	55.40	63.28	71.19

Stream Basin	Channel Gradient	Mean Channel Width	Mean Channel Depth	Mean Channel Area	Mean Volume of Bed Material	Channel Length
Beetree	430.38	36.50	6.19	272.76	37.45	3.16
Noland	312.61	24.00	3.42	102.96	14.61	7.46
Turtletown	47.48	22.60	10.68	280.36	.96	5.13
Davidson	57.36	74.67	9.72	756.80	11.41	10.23
Hiawassee	60.28	40.67	5.53	272.90	10.51	9.62
Cataloochee	33.78	68.83	11.83	833.18	2.19	11.25
Scott	112.40	49.83	8.05	406.27	.94	11.97
Nantahale	42.75	73.00	8.22	579.97	1.93	14.58
Jonathan	65.70	64.50	12.38	758.06	5.78	18.79
Mills	58.78	51.33	8.23	53.33	5.08	25.93
French Broad	83.24	71.67	10.28	856.01	1.60	17.32
Fightingtown	36.35	45.53	6.19	332.32	2.31	28.62
Nottely	39.80	46.42	8.49	459.55	6.09	11.39
Hominy	96.36	46.33	8.66	442.57	1.40	12.34
Collasaja	134.90	64.83	15.22	1027.39	12.58	19.33
Watauga	69.60	82.67	7.10	725.43	94.71	17.08
Valley	37.31	50.77	7.10	451.34	1.37	22.59
Tellico	91.75	72.57	3.94	295.62	47.43	26.83
Big Laurel	66.30	58.33	7.74	501.83	2.25	28.80
Pigeon	92.46	82.33	23.44	2696.26	1.80	24.20
Doe	59.36	72.33	5.74	469.31	.98	27.50
Little Tennessee	6.12	64.33	9.45	689.38	.87	25.18
Cane	33.98	80.67	10.83	876.73	2.47	39.15
Ivy	38.18	60.00	7.89	536.48	40.51	24.37
Toccoa	15.30	71.00	9.75	818.42	7.87	26.58

Table 2. Correlation Matrix.

	Gradient	Width	Depth	Area	Material	Length
$Q_{2.33}$	.153	-.157	-.147	-.182	-.338	-.222
Q_5	.099	-.278	.185	-.358	-.240	.131
Q_{10}	.341	.127	.012	.009	.294	-.123
Q_{25}	.360	.101	.012	-.009	.289	-.104
Q_{50}	.341	.112	.002	-.009	.277	-.090
Q_{100}	.375	.134	.044	-.018	.299	-.089

variables are calculated somewhat differently from those in other studies. The rationale for any deviation from previously established measurements is purely subjective; but with emphasis placed on ease, simplicity and a minimum of interpretation. In addition, channel length was included because of its relationship to the other hydraulic variables and drainage basin dimensions.

TEST OF THE WORKING HYPOTHESES

To illustrate the previously mentioned problems and to test the working hypotheses, a multiple linear regression model was employed (Ezikel & Fox, 1959). Step-wise regression analysis was used, which eliminates the insignificant independent variables at the 0.05 level of confidence by employing the F-statistic. The purpose for using the step-wise method was to analyze only those variables which were significantly contributing to the explanation of the variation of the dependent variables.

The simple correlation of the flood frequencies and the channel variables reveals the importance of each channel variable on the flood frequency variables (Table 2). At the 0.05 level of confidence no independent variable is significant in predicting the variability of a single flood frequency. However, certain relationships are shown. For example, the correlation coefficients (r-values) vary on the ordinate as well as the abcissa in the matrix. This is particularly the case with channel gradient which increases its r-value as flood frequency increases. On the other hand, the r-values seem to vary in magnitude without any apparent pattern as expected.

The results of the step-wise regression analysis are shown in Table 3. The R-value is the multiple correlation coefficient and the D-value is the coefficient of determination. The R-value is similar to the r-value above except that more than one independent variable is used in attempting to explain the differences in the dependent variables. The square of the coefficient of multiple correlation is the coefficient of determination (D-value) which is the percentage to which the variance

Table 3. Relationship Between Flood Frequencies and Channel Variables.

For $Q_{2.33}$	R	D	For Q_{25}	R	D
Material	.338	.114	Gradient	.360	.116
Gradient	.447	.200	Width	.499	.249
Length	.493	.244	Material	.526	.276
Area	.544	.296	Length	.544	.296
Depth	.560	.313	Area	.553	.306
For Q_5			For Q_{50}		
Area	.358	.128	Gradient	.341	.116
Material	.487	.237	Width	.486	.236
Depth	.533	.284	Material	.511	.261
Width	.577	.333	Length	.528	.278
Length	.595	.354	Area	.535	.286
For Q_{10}			For Q_{100}		
Gradient	.341	.116	Gradient	.375	.140
Width	.499	.249	Width	.543	.295
Material	.529	.280	Material	.569	.324
Length	.551	.304	Length	.584	.341
Area	.562	.316	Area	.591	.349
			Depth	.594	.352

of the dependent variable is explained by the independent variables.
For example, in Table 3, 31.3 percent of the variation in the mean
annual flood is determined by all the independent variables which re-
mained in the model. This can be stated because the D-value measures
that proportion of all the elements of variation in the mean annual flood
that are also present in the independent variables. But it must be re-
membered that a change in the sample size or number of variables will
contribute to a change in the statistics!

These statistical analyses show a functional relationship between
the flood frequencies and the channel variables. To test the variation
of these relationships, standardized residuals from regression must be
employed. The standardized residual is expressed as

$$S_r = \frac{Ye - Yo}{Sy_e}$$

where Ye is the computed estimate of the residual from regression, Yo
is the observed value, and Sy_e is the standard error of estimate
(Thomas, 1960). This expression offers a value for the difference
between the estimated and observed deviation from the regression sur-
face for a single case in a set of observations in terms of the standard

171

error of estimate. The standard error of estimate is a value which measures the closeness with which the estimated values agree with the original values.

The first hypothesis stated that the relationship between the flood frequencies and the channel factors varied from one basin to another. Table 4, which is a matrix showing the standardized residuals from regression, reveals that a considerable number of cases is beyond the ± 0.5 standard error for the various flood frequencies; in fact, three do not show a "hit" or a value less than ± 0.5 for any flood frequency. Two basins hit within ± 0.5 standard error for every flood, while four basins hit five out of six times. Obviously, due to the mix and the variation of the residual values, the hypothesis stated above is accepted; that is, the relationship does vary from basin to basin.

The second hypothesis stated that the variation between floods and channel variables tends to change as flood magnitude increases. Again, by using the residual matrix in Table 4, it can be ascertained that a change takes place as flood magnitude increases. With regard to mean annual flood, for example, fourteen out of the twenty-five cases were within ± 0.5 standard error of the regression surface. This compares with eight hits in the 10-year flood. As one can observe, there is a sharp break between the 5-year and the 10-year flood. This break also relates to the sequential change in channel variables noted earlier in Table 3.

Overall, the matrix indicates that 42 percent of the observations for the different floods were within ± 0.5 standard error of the regression surface. Approximately 27 percent of the same observations were beyond ± 1 standard error. Theoretically this will occur about 32 percent of the time. From the matrix then, the second hypothesis is also accepted since change does take place in the variables as the flood frequencies decrease. It has been shown from the analysis that the relationships which were established in the regression analysis do in fact vary from basin to basin, in addition to varying as flood magnitude increases.

CONCLUSIONS

In conclusion, two observations must be stressed as a result of the testing procedure. First, that the standardized residuals from regression indicate variation from basin to basin with regard to the regression analysis. Second, that the residual matrix reveals that a break exists between the 5-year and 10-year floods with regard to deviation from the regression surface. These two observations should indicate the necessity to make appropriate adjustments when predicting floods.

In order to create more reliable predictions, it is suggested that those streams which are extreme cases, as indicated by the

Table 4.   Standardized Residuals From Regression.

Ident. No.	Stream Name	on $Q_{2.33}$	on Q_5	on Q_{10}	on Q_{25}	on Q_{50}	on Q_{100}	Total Under .5
1	Beetree	.461	.302	.913	.931	.959	.962	2
2	Noland	.693	.258	-.628	-.590	-.726	-.995	1
3	Turtletown	-1.430	-.986	-1.090	-1.170	-1.223	-1.128	0
4	Davidson	.597	-.770	.200	.172	.167	.039	4
5	Hiawassee	.865	.421	.568	.524	.589	.696	1
6	Cataloochee	-.332	1.120	-.198	-.170	-.170	-.141	5
7	Scott	-1.147	-.621	-1.234	-1.220	-1.167	-.583	0
8	Nantahala	.561	.338	.057	-.038	-.081	-.264	5
9	Jonathan	.222	.388	-1.530	-1.574	-1.582	-1.730	2
10	Mills	-.278	-.358	.757	.755	.756	.716	2
11	French Broad	.334	-1.556	.893	.845	.818	.869	1
12	Fightingtown	.320	-.327	.272	.185	.320	.409	6
13	Nottely	.390	.627	.091	-.006	-.041	-.129	5
14	Hominy	-.819	-.194	-.171	-.041	.029	-.087	5
15	Cullasaja	-.292	-.073	.079	.089	.104	-.013	6
16	Watauga	-3.177	-2.481	1.874	1.847	1.812	1.676	0
17	Valley	.102	.362	1.166	1.190	1.167	1.164	2
18	Tellico	1.017	1.220	-1.150	-1.187	-1.180	-.413	1
19	Big Laurel	.013	-.280	-.542	-.499	-.478	-.653	4
20	Pigeon	.574	1.190	.335	.293	.281	.109	4
21	Doe	.039	.134	.517	.565	.562	.447	3
22	Little Tennessee	-.109	-.652	.581	.655	.612	.686	1
23	Cane	.425	1.447	.719	.812	.812	.892	1
24	Ivy	.355	.542	-1.370	-1.215	-1.143	-1.215	1
25	Toccoa	.617	-.049	-1.108	-1.155	-1.194	-1.314	1
	Total under .5	14	13	8	9	9	10	

standardized residuals, be eliminated from the model. Or, at least one should refrain from predicting floods on those streams using the same independent variables which were in the regression model. Of course, those basins that are within ± 0.5 standard error of the regression surface should remain in the model. Flood prediction on these basins should be quite accurate.

With regard to the second observation, it is apparent that the accuracy of flood prediction decreases as flood magnitude increases. That is, predicting a flood magnitude which theoretically occurs every 100 years will be less accurate than predicting a flood magnitude which occurs every five years. In regional flood analysis, the accuracy of predicting floods on certain streams beyond the 5-year flood could be unfavorable.

As previously mentioned, the results of a regression analysis depends greatly on the number and nature of the independent variables entered into the model when predicting floods. Thus, it is suggested that standardized residuals from regression be used in order to eliminate deviate basins from the analysis. This will insure a more accurate picture of floods on a regional basis, and point out those basins which need additional analysis.

REFERENCES CITED

Benson, M. A., 1962, Factors influencing the occurrence of floods in a humid region of diverse terrain: U. S. Geological Survey Water Supply Paper 1580-B.

Ezikel, Mordecai, and Fox, K. A., 1959, Methods of correlation and
    regression analysis: New York, John Wiley.
Kazman, Raphael G., 1965, Modern hydrology: New York; Harper and
    Row, p. 63.
Leopold, L. B., and Maddock, T., 1953, The hydraulic geometry of
    stream channels and some physiographic implications: U. S.
    Geological Survey Prof. Paper 252, p. 25.
Thomas, E. N., 1960, Maps of residuals from regression: Their
    characteristics and uses in geographic research: Dept. of Geo-
    graphy, Monograph No. 2, University of Iowa, Iowa City, p. 21-
    24.
Wolman, M. G., 1955, The natural channel of Brandywine Creek,
    Pennsylvania: U. S. Geological Survey Prof. Paper 271, p. 10.
Wong, Shoe Tuck, 1963, A multivariate statistical model for predicting
    mean annual flood in New England: Annals of the Assoc. of Am.
    Geographers, v. 53.

BIBLIOGRAPHY AND LIST (1900-1965) OF THE FAMILIES

CONSTELLARIIDAE AND DIANULITIDAE

(ECTOPROCTA, ORDER CYSTOPORATA)

By

Frank K. McKinney
Department of Geography and Geology
Appalachian State University
Boone, North Carolina 28607

ABSTRACT

This paper is a bibliography and list of taxa for the families Constellariidae and Dianulitidae covering the years 1900 to 1965. Family-group taxa are in a separate list from genus- and species-group taxa.

INTRODUCTION

The families Constellariidae and Dianulitidae were originally erected as families belonging to the ectoproct order Trepostomata. Astrova (1964) erected the order Cystoporata to receive the Paleozoic ectoproct families Ceramoporidae and Fistuliporidae from the order Cyclostomata and the families Constellariidae and Dianulitidae from the order Trepostomata. In accordance with this concept of classification of Paleozoic ectoprocts, this bibliography and list of constellariids and dianulitids was extracted from a larger bibliography and list of Trepostomata for the years 1900-1965, which is to be published in a later paper. Textbooks and stratigraphic lists are not included in the bibliography.

J. M. Nickles and R. S. Bassler coauthored "A synopsis of American fossil Bryozoa including bibliography and synonymy" in 1900, which was published as Bulletin 173 of the United States Geological Survey. The small bibliography and taxonomic list presented here is intended as a supplement to their work for the Constellariidae and Dianulitidae. The publications examined for the present compilation are from world-wide paleontologic literature, whereas Nickles and Bassler restricted themselves to literature relating to North American ectoprocts.

Pertinent papers were extracted from the literature by examination of all Paleozoic ectoproct literature listed in the Bibliography of North American Geology, the Bibliography of Geology Exclusive of

North America and the Zoological Record covering the years up through
1965. In addition, lists of references cited at the end of all papers
found were examined so that literature missed in the standard biblio-
graphies could be included.

Taxa are recorded as they were listed in the literature. No
attempt to judge validity or correctness of the generic assignment of
species is made. References to alphabetically listed family-group
taxa are placed spearately from references to genus- and species-group
names (also listed alphabetically), so that no implication of classifica-
tion below subfamily rank is given. Geologic period is indicated for
each species. Designation of geologic period is not meant to imply that
the species ranges throughout the period, rather that the species has
been reported from rocks of that period. Country from which the types
were described follows indication of geologic period for each species.

This paper had its origin in a reading course under the direction
of Joseph St. Jean, University of North Carolina at Chapel Hill. His
support and encouragement are gratefully acknowledged. My wife,
Margie Jackson McKinney, helped track down obscure publications.
Thanks are also due Richard S. Boardman of the U. S. National
Museum who critically read the manuscript.

REFERENCES TO FAMILIES AND SUBFAMILIES (1900-1965)

Family Constellariidae Ulrich, 1890. Bassler, 1911, p. 218: Coryell,
    1921, p. 288: Bassler, 1953, p. 105: Astrova et al., 1960, p.
    59: Boardman, 1960, p. 25: Astrova, 1964, p. 30 (translated
    1965, p. 1627): Astrova, 1965, p. 134, 135.
    Subfamily Constellariinae Vinassa de Regny, 1920, p. 218.
    Subfamily Revaloporinae Vinassa de Regny, 1920, p. 220.
Family Dianulitidae Vinassa de Regny, 1920, p. 224: Astrova, 1964,
    p. 29 (translated 1965, p. 1627): Astrova, 1965, p. 131, 132.

REFERENCES TO GENERA AND SPECIES (1900-1965)

Constellaria Dana, 1846. Cumings, 1908, p. 742, 743: Bassler, 1911,
    p. 218, 219: Vinassa de Regny, 1920, p. 218: Coryell, 1921, p.
    288, 289: McFarlan, 1931, p. 100: Bassler, 1935a, p. 78:
    Bassler, 1953, p. 105, 106: Astrova, et al., 1960, p. 59:
    Yaroshinskaya, 1960, p. 395: Ross, 1963, p. 51-54: Ross, 1964,
    p. 934, 937, 938, 943, 944, 946: Astrova, 1965, p. 140.
    Constellaria antheloidea (Hall, 1847). Ross, 1963, p. 54, Pl.
        5, figs. 1, 3-6, 8, Pl. 6, fig. 5. (Stellipora antheloidea
        Hall, 1847) Ordovician. U.S.A.
    Constellaria cambrensis Lewis, 1933, p. 593-595, Text-figs.
        a, b. Ordovician. Great Britain.

Constellaria constellata (Van Cleve in Dana, 1846). Cumings,
1908, p. 804, 805, Pl. 12, fig. 4-4e, Pl. 27, fig. 19:
Bassler, 1953, Text-fig. 71, 1a-e. (Ceriopora constellata
Van Cleve in Dana, 1846) Ordovician. U.S.A.

Constellaria constellata var. prominens Ulrich, 1883. Cumings,
1908, p. 806, Pl. 27, fig. 18. Ordovician. U.S.A.

Constellaria emaciata Ulrich and Bassler, 1904. Nickles, 1905,
p. 44, 45, Pl. 1, fig. 7, 8: McFarlan, 1931, p. 101, Pl. 7,
fig. 3.
(Constellaria florida var. emaciata Ulrich and Bassler,
1904) Ordovician. U.S.A.

Constellaria fischeri Ulrich, 1883. McFarlan, 1931, p. 101,
102, Pl. 6, figs.3, 4. Ordovician. U.S.A.

Constellaria florida Ulrich, 1882. Nickles, 1905, p. 54, 55,
Pl. 3, fig. 5: McFarlan, 1931, p. 100, 101, Pl. 6, figs. 1,
2, Pl. 10, fig. 1. Ordovician. U.S.A.

Constellaria florida var. emaciata Ulrich and Bassler, 1904,
p. 37, 38. (see also Constellaria emaciata) Ordovician. USA.

Constellaria floridaeformis Yaroshinskaya, 1960, p. 395, Pl.
0-14, fig. 4a, Pl. 0-15, fig. 2a. Ordovician. U.S.S.R.
(Siberia)

Constellaria islensis Ross, 1963, p. 54-56, Pl. 5, figs. 2, 7,
9, 10, Pl. 6, figs. 1-4, 6-8. Ordovician. U.S.A.

Constellaria lamellosa Coryell, 1921, p. 289. Pl. 7, fig. 3-5.
Ordovician. U.S.A.

Constellaria limitaris (Ulrich, 1879). Cumings, 1908, p. 806-
808, Pl. 13, fig. 2, Pl. 28, fig. 2: McFarlan, 1931, p.
102. (Stellipora limitaris Ulrich, 1879) Ordovician. U.S.A.

Constellaria cf. C. limitaris (Ulrich, 1879). Dyer, 1925, p. 52,
Pl. 6, fig. 6. Ordovician.

Constellaria polystomella Nicholson, 1875. Cumings, 1908, p.
808, 809, Pl. 13, fig. 1-1b, Pl. 18, fig. 1: Foerste, 1924,
p. 106, Pl. 9, fig. 1: Dyer, 1925, p. 52: McFarlan, 1931,
p. 102, Pl. 14, fig. 17: Utgaard and Perry, 1964, p. 88-
90, Pl. 17, figs. 8, 9, Pl. 18, fig. 1. Ordovician. U.S.A.

Constellaria prominens Ulrich, 1883. Nickles, 1905, p. 52, Pl.
2, fig. 15. Ordovician. U.S.A.

Constellaria cf. C. punctata (Whitfield, 1882). Utgaard and
Perry, 1964, p. 90, 91, Pl. 18, figs. 2, 3. (Monticulipora
punctata Whitfield, 1882) Ordovician. U.S.A.

Constellaria teres Ulrich and Bassler, 1904, p. 37: McFarlan,
1931, p. 100, Pl. 4, fig. 12. Ordovician. U.S.A.

Constellaria varia Ulrich, 1893. Bassler, 1911, p. 219-221,
Text-figs. 120a-e, 121a, b, 122a, b: Sardeson, 1936, p.
339, Pl. 30, fig. 6: Fritz, 1957, p. 13, Pl. 5, figs. 4, 5:
Astrova et al., 1960, Text-fig. 67a, b: Astrova, 1965, p.
441, Pl. 7, fig. 2a-c. Ordovician. U.S.A.

Dianulites Eichwald, 1829. Bassler, 1911, p. 226-229: Vinassa de
      Regny, 1920, p. 224: Bassler, 1935a, p. 92: Astrova, 1940,
      p. 59: Astrova, 1945, p. 87, 88: Astrova, 1951, p. 131: Bassler,
      1953, p. 106: Modzalevskaya, 1953, p. 132, 133: Astrova et al.,
      1960, p. 60: Astrova, 1965, p. 132.

Dianulities apiculatus (Eichwald, 1829). Mannil, 1961, p. 125,
      126, Pl. 4, figs. 2, 3, Pl. 5, fig. 1, Text-fig. 3. Ordovi-
      cian. U. S. S. R.

Dianulites borealis Astrova, 1965, p. 133, Pl. 4, fig. 2a, b.
      Ordovician. U. S. S. R.

Dianulites collifera Bassler, 1911, p. 239, 240, Text-fig. 134a-
      f. Ordovician. U. S. S. R.

Dianulites fastigiatus Eichwald, 1829. Bassler, 1911, p. 229-
      232, Pl. 2, figs. 1-3, Text-figs. 127a-d, 128a-d: Bassler,
      1953, Text-fig. 71, 3a-e: Astrova et al., 1960, Text-fig.
      69a, b: Mannil, 1961, Pl. 1, fig. 1. Ordovician. U. S. S. R.

Dianulites globularis Bassler, 1928, p. 152, Pl. 9, figs. 6-8.
      Ordovician. Canada

Dianulites grandis Bassler, 1911, p. 237, 238, Text-fig. 133a-
      e. Ordovician. U. S. S. R.

Dianulites hexaporites Pander, 1830. Modzalevskaya, 1953, p.
      134-138, Pl. 8, figs. 1-4, Text-fig. 17. (see also Dianulites
      petropolitana var. hexaporites) Ordovician. U. S. S. R.

Dianulites insueta Bassler, 1928, p. 151, Pl. 7, fig. 8, Pl. 9,
      figs. 3-5. Ordovician. Canada.

Dianulites janischevskyi Modzalevskaya, 1953, p. 138-140, Pl.
      7, figs. 5, 6, Text-fig. 18: Astrova, 1965, p. 132, 133,
      Pl. 4, fig. 1a, b. Ordovician. U. S. S. R.

Dianulites (?) kossjensis Astrova, 1940, p. 61-63, 80, 81, Pl.
      8, figs. 1-3, Pl. 9, figs. 1-4. Ordovician. U. S. S. R.

Dianulites maculatus Modzalevskaya, 1953, p. 133, 134, Pl. 7,
      figs. 1-4, Text-fig. 16. Ordovician. U. S. S. R.

Dianulites magnicellularis Modzalevskaya, 1953, p. 141-143,
      Pl. 9, figs. 1-3, Text-fig. 20. Ordovician. U. S. S. R.

Dianulites microcellatus Astrova, 1945, p. 88, 89, 92, Pl. 12,
      figs. 3, 4, Text-fig. 3. Ordovician. U. S. S. R.

Dianulites multimesoporicus Modzalevskaya, 1953, p. 140, 141,
      Pl. 8, figs. 5, 6, Text-fig. 19. Ordovician. U. S. S. R.

Dianulites petropolitana Dybowski, 1877. Bassler, 1911, p.
      232-237, Pl. 2, figs. 4, 5, Pl. 10, figs. 7, 11, Text-figs.
      129a-c, 130a-d, 131a-f, 132a-c: Bassler, 1919, p. 217,
      218, Pl. 44, figs. 6, 7: Sardeson, 1936, p. 183: Astrova,
      140, p. 59-61, 80, Pl. 7, figs. 1-5: Sissingh, 1965, p. 161,
      Pl. 1, figs. 4, 5, Pl. 3, figs. 8, 9. Ordovician. U. S. S. R.

Dianulites aff. D. petropolitana Dybowski, 1877. Ozaki, 1933,
      p. 116, Pl. 9, figs. 1, 2, Pl. 10, figs. 1, 2. Ordovician.

Dianulites petropolitana var. hexaporites Pander, 1830. Bassler,

1911, Pl. 2, fig. 6, 6a. (see also Dianulites hexaporites)
Ordovician. U.S.S.R.

Dianulites petropolitana var. minor Lewis, 1934, p. 103, Pl. 7,
fig. 10a, b. Ordovician. Great Britain.

Dianulites petropolitana var. sibiricus Astrova, 1951, p. 132,
Pl. 1, fig. 6, Text-fig. 3a, b. Ordovician. U.S.S.R.

Dianulites preinsuetus Astrova, 1965, p. 134, Pl. 5, fig. 1a, b.
Ordovician. U.S.S.R.

Dianulites rocklandensis Wilson, 1921, p. 47, Pl. 2, figs. 1,
2: Fritz, 1957, p. 15. Ordovician. Canada.

Dianulites yumensis Yang and Loo, 1962, p. 51, Pl. 9, figs. 1-
3. Ordovician? China

Dianulites sp. Roy, 1941, p. 82, 83, Text-fig. 44a-d: Welby,
1962, Pl. 4, figs. 9-11.

Hennigopora Bassler, 1952, p. 382: Bassler, 1953, p. 106: Astrova,
1965, p. 141, 142.

Hennigopora apta Perry and Hattin, 1960, p. 704, 705, Pl. 88,
figs. 1, 3, 4. Silurian. U.S.A.

Hennigopora florida (Hall, 1852). Bassler, 1953, Text-fig. 71,
2a-d. (Callopora florida Hall, 1852) Silurian. U.S.A.

Hennigopora floridiformis Astrova, 1965, p. 142, 143, Pl. 8,
fig. 1a, b, Text-fig. 29a, b. Silurian. U.S.S.R.

Idiotrypa Ulrich, 1883. Bassler, 1906, p. 39: Vinassa de Regny, 1920,
p. 224: Bassler, 1935a, p. 131: Bassler, 1953, p. 106.

Idiotrypa parasitica Ulrich, 1883. Bassler, 1953, Text-fig. 71,
4a-c. Silurian. U.S.A.

Idiotrypa punctata (Hall, 1852). Bassler, 1906, p. 40, Pl. 17,
figs. 4-10, Pl. 24, figs. 17-19. (Trematopora ?? punctata
Hall, 1852) Silurian. U.S.A.

Revalopora Vinassa de Regny, 1920, p. 220: Bassler, 1935a (equals
Stellipora), p. 189: Bassler, 1953 (equals Stellipora), p. 107.

Revalotrypa Bassler, 1952, p. 382: Bassler, 1953, p. 107.

Revalotrypa gibbosa (Bassler, 1911). Bassler, 1953, Text-fig.
72, 1a-e. (Nicholsonella gibbosa Bassler, 1911, p. 224-226,
Pl. 11, figs. 1-6, Text-figs. 125a, b, 126a-i) Ordovician.
U.S.S.R.

Stellipora Hall, 1847. Bassler, 1911, p. 221: Vinassa de Regny, 1920,
p. 218, 219: Bassler, 1935a, p. 206: Bassler, 1953, p. 107:
Astrova et al., 1960, p. 59, 60: Yaroshinskaya, 1960, p. 395:
Kiepura, 1962, p. 384: Astrova, 1965, p. 137, 138.

Stellipora antheloidea Hall, 1847. Sardeson, 1901, p. 14, 15:
Bassler, 1953, Text-fig. 72, 2a-d. Ordovician. U.S.A.

Stellipora apsendesoides Bassler, 1911, p. 223, 224, Text-fig.
124: Bassler, 1953, Text-fig. 72, 3. Ordovician. U.S.S.R.

Stellipora complicata Astrova, 1965, p. 139, 140, Pl. 7, fig.
la, b. Ordovician. U. S. S. R.

Stellipora constellata Dybowski, 1877. Bassler, 1911, p. 223,
Pl. 4, fig. 9, 9a. Ordovician. U. S. S. R.

Stellipora corticosa (Ulrich, 1886). Sardeson, 1936, p. 340-342,
344-346, Pl. 30, figs. 7-9. (Phyllopora? corticosa Ulrich,
1886) Ordovician. U. S. A.

Stellipora revalensis Dybowski, 1877. Bassler, 1911, p. 221-
223, Pl. 4, fig. 8-8b, Text-fig. 123a, b: Astrova et al.,
1960, Text-fig. 68a, b. Ordovician. U. S. S. R.

Stellipora stipata Bassler, 1932, Pl. 11, figs. 3, 4: Bassler,
1935b, p. 406. Ordovician. U. S. A.

Stellipora vesiculosa Modzalevskaya in Modzalevskaya and Nek-
horoshev, 1955, p. 53, 54, Pl. 38, fig. 1: Yaroshinskaya,
1960, p. 396, Pl. 0-15, fig. la, b: Kiepura, 1962, p. 385,
386, Pl. 3, fig. 2: Astrova, 1965, p. 138, 139, Pl. 5, fig.
3, Pl. 6, fig. la-d, Text-fig. 28. Ordovician. U. S. S. R.

Xenotrypa Bassler, 1952, p. 381, 382: Bassler, 1953, p. 87, Astrova,
1965, p. 135, 136.

Xenotrypa bassleri Astrova, 1965, p. 136, 137, Pl. 5, fig. 2a,
b, Text-fig. 27. Ordovician. U. S. S. R.

Xenotrypa primaeva (Bassler, 1911). Bassler, 1953, Text-fig.
51, 6a, b. (Fistulipora primaeva Bassler, 1911, p. 109-
111, Text-fig. 40a-e) Ordovician. U. S. S. R.

INDEX OF TRIVIAL NAMES[1]

antheloidea, Constellaria
           Stellipora
apiculatus, Dianulites
apsendesoides, Stellipora
apta, Hennigopora
bassleri, Xenotrypa
borealis, Dianulites
cambrensis, Constellaria
collifera, Dianulites
complicata, Stellipora
constellata, Ceriopora
           Constellaria
           Stellipora
constellata prominens, Constellaria
corticosa, Phyllopora?
           Stellipora

emaciata, Constellaria
fastigiatus, Dianulites
fischeri, Constellaria
florida, Callopora
           Constellaria
           Hennigopora
florida emaciata, Constellaria
floridaeformis, Constellaria
floridiformis, Hennigopora
gibbosa, Nicholsonella
           Revalotrypa
globularis, Dianulites
grandis, Dianulites
hexaporites, Dianulites
insueta, Dianulites
islensis, Constellaria

1/ Including names assigned to genera of the Constellariidae and Dia-
nulitidae between 1900 and 1965 and names of genera to which
species were originally assigned.

janischevskyi, Dianulites
kossjensis, Dianulites (?)
lamellosa, Constellaria
limitaris, Constellaria
            Stellipora
maculatus, Dianulites
magnicellularis, Dianulites
microcellatus, Dianulites
multimesoporicus, Dianulites
parasitica, Idiotrypa
petropolitana, Dianulites
petropolitana hexaporites, Dianulites
petropolitana minor, Dianulites
petropolitana sibiricus, Dianulites
polystomella, Constellaria

preinsuetus, Dianulites
primaeva, Fistulipora
            Xenotrypa
punctata, Constellaria
            Idiotrypa
            Monticulipora
            Trematopora? ?
revalensis, Stellipora
rocklandensis, Dianulites
stipata, Stellipora
teres, Constellaria
varia, Constellaria
vesiculosa, Stellipora
yumenensis, Dianulites

BIBLIOGRAPHY

Astrova, G. G., 1940, Nizhnesiluriĭskie Trepostomata basseĭna Pechory: Moskov. Gosud. Ped. Inst. Uchenye Zapiski, v. 23, Kafedra Geologii, no. 2, 82 p., 13 pls.

_____, 1945, Nizhnesiluriĭskie Trepostomata reki Kozhima: Vser. Paleont. Obshch. Ezhegodnik, v. 12, p. 81-92, pl. 12.

_____, 1951, Pervye nakhodki nizhnesiluriĭskikh Trepostomata v Sibiri: Moskov. Obshch. Ispytateley Prirody Byull., Otdel Geol. Trudy, v. 1, p. 128-135, 1 pl.

_____, 1964, O novom otryade paleozoiskikh mshanok: Paleont. Zhurnal, no. 2, p. 22-31. (Translated 1965, A new order of Paleozoic Bryozoa: Internat. Geology Rev., v. 7, p. 1622-1628).

_____, 1965, Morfologiya, istoria razvitiya i sistema ordovikskikh i siluriiskikh mshanok: Akad. Nauk SSSR Paleont. Inst. Nauk Trudy, v. 106, 431 p., 84 pls.

_____, et al., 1960, Tip Bryozoa, in Sarycheva, T. G., ed., Osnovy paleontologii mshanki, brakhiopody: Akad. Nauk SSSR Osnovy Paleontologii, v. 7, p. 15-111, 7 pls.

Bassler, R. S., 1906, The bryozoan fauna of the Rochester shale: U.S. Geol. Survey Bull. 292, 136 p., 31 pls.

_____, 1911, The early Paleozoic Bryozoa of the Baltic provinces: U. S. Natl. Mus. Bull. 77, 382 p., 13 pls.

_____, 1919, Cambrian and Ordovician: Maryland Geol. Survey, 424 p., 58 pls.

_____, 1928, Bryozoa, in Twenhofel, W. H., Geology of Anticosti Island: Canada Geol. Survey Mem. 154, p. 143-168, pls. 1, 5-14.

_____, 1932, The stratigraphy of the Central Basin of Tennessee: Tennessee Div. Geology Bull. 38, 268 p., 49 pls.

Bassler, R. S., 1935a, Bryozoa: Fossilium Catalogus; I, Animalia, pt. 67, 229 p.

_____, 1935b, Descriptions of Paleozoic fossils from the Central Basin of Tennessee: Washington Acad. Sci. Jour., v. 25, p. 403-409.

_____, 1952, Taxonomic notes on genera of fossil and Recent Bryozoa: Washington Acad. Sci. Jour., v. 42, p. 381-385, 27 text-figs.

_____, 1953, Bryozoa, in Moore, R. C., ed., Treatise on invertebrate paleontology, pt. G: Geol. Soc. America and Univ. Kansas Press, 253 p., 175 text-figs.

Boardman, R. S., 1960, Trepostomatous Bryozoa of the Hamilton Group of New York State: U. S. Geol. Survey Prof. Paper 340, 87 p., 22 pls.

Coryell, H. N., 1921, Bryozoan faunas of the Stones River group of central Tennessee: Indiana Acad. Sci. Proc. for 1919, p. 261-340, 14 pls.

Cumings, E. R., 1908, The stratigraphy and paleontology of the Cincinnatian series of Indiana: Indiana Dept. Geology Ann. Rept. 32, p. 605-1188, 55 pls.

Dyer, W. S., 1925, The stratigraphy and paleontology of Toronto and vicinity; Pt. 5, The paleontology of the Credit River section: Ontario Dept. Mines Ann. Rept. 32, pt. 7, p. 47-88, 7 pls.

Foerste, A. F., 1924, Upper Ordovician faunas of Ontario and Quebec: Canada Geol. Survey Mem. 138, 251 p., 46 pls.

Fritz, M. A., 1957, Bryozoa (mainly Trepostomata) from the Ottawa formation (Middle Ordovician) of the Ottawa-St. Lawrence Lowland (Ottawa-Quebec): Canada Geol. Survey Bull. 42, 75 p., 30 pls.

Kiepura, Maria, 1962, Bryozoa from the Ordovician erratic boulders of Poland: Acta Palaeont. Polonica, v. 7, p. 347-428, 11 pls.

Lewis, H. P., 1933, The genus Constellaria Dana in Britain: Annals and Mag. Nat. History, v. 12, p. 591-595, text-figs. a, b.

_____, 1934, The occurrence of fossiliferous pebbles of Salopian age in the Peel Sandstones (Isle of Man): Great Britain Geol. Survey Summ. Prog. 1933, pt. 2, p. 91-108, pls. 6-8.

Mannil, R. M., 1961, K morfologii polusfericheskikh mshanok otryada Trepostomata: Eesti Nsv Teaduste Akad. Geol. Inst., Uurimused 6, p. 113-140, 8 pls.

McFarlan, A. C., 1931, The Ordovician fauna of Kentucky, in Jillson, W. R., ed., Paleontology of Kentucky: Kentucky Geol. Survey Rept., ser. 6, v. 36, p. 47-165, pls. 1-16.

Modzalevskaya, E. A., 1953, Trepostomaty ordovika Pribaltiki i ikh stratigraficheskoe znachenie: Vses. Neft. Nauchno-Issled. Geol.-Razved. Inst. Sbornik, v. 78, p. 91-167, 14 pls.

_____, and Nekhoroshev, V. P., 1955, Klass Bryozoa mshanki, in Polevoi atlas ordovikskoi i siluriiskoi fauny Sibirskoi plat-

formy: Vses. Nauchno-Issled. Geol. Inst., p. 48-60, pls. 11, 12, 24-26, 38, 39, 55, 56.

Nickles, J. M., 1905, The Upper Ordovician rocks of Kentucky and their Bryozoa: Kentucky Geol. Survey Bull. 5, 64 p., 3 pls.

Ozaki, Kin-emon, 1933, On two species of Ordovician Bryozoa from south Manchuria: Japanese Jour. Geology and Geography, v. 10, p. 115-117, pls. 9, 10.

Perry, T. G. and Hattin, D. E., 1960, Osgood (Niagaran) bryozoans from the type area: Jour. Paleontology, v. 34, p 695-710, pls. 85-90.

Ross, J. R. P., 1963, Constellaria from the Chazyan (Ordovician), Isle la Motte, Vermont: Jour. Paleontology, v. 37, p. 51-56, pls. 5, 6.

_____, 1964, Morphology and phylogeny of early Ectoprocta (Bryozoa): Geol. Soc. America Bull., v. 75, p. 927-948, 10 text-figs.

Roy, S. K., 1941, The Upper Ordovician fauna of Frobisher Bay, Baffin Land: Field Mus. Nat. History Geol. Ser. Mem. 2, 212 p., 146 text-figs.

Sardeson, F. W., 1901, Problem of the Monticuliporoidea. I: Jour. Geology, v. 9, p. 1-27, pl. A.

_____, 1936, Early bryozoans; Monotrypa and Eridotrypa: Pan-Am. Geologist, v. 66, p. 179-190, pl. 15.

Sissingh, W., 1965, Grote paleozoische bryozoen uit het Keil'eem: Natuurhistorisch Maandblad, v. 54, p. 155-171, 4 pls.

Ulrich, E. O. and Bassler, R. S., 1904, A revision of the Paleozoic Bryozoa. Pt. II - On genera and species of Trepostomata: Smithsonian Misc. Coll., v. 47, p. 15-55, pls. 6-14.

Utgaard, John and Perry, T. G., 1964, Trepostomatous bryozoan fauna of the upper part of the Whitewater Formation (Cincinnatian) of eastern Indiana and western Ohio: Indiana Geol. Survey Bull. 33, 111 p., 23 pls.

Vinassa de Regny, P. E., 1920, Sulla classificazione dei treptostomidi: Italiana Soc. Sci. Nat. Atti, v. 59, p. 212-231.

Welby, C. W., 1962, Paleontology of the Champlain Basin in Vermont: Vermont Geol. Survey Spec. Publ. 1, 88 p., 16 pls.

Wilson, A. E., 1921, The range of certain Lower Ordovician faunas of the Ottawa Valley with descriptions of some new species: Canada Dept. Mines, Geol. Survey Bull. 33, p. 19-57, pls. 2-4.

Yang, King-chih and Loo, L. H., 1962, Paleozoic bryozoan fossils of the K'ilien Mountains: Acad. Sinica Inst. Geology and Palaeontology, Geology of the K'ilien Mountains, v. 4, pt. 5, p. 1-114, 24 pls.

Yaroshinskaya, A. M., 1960, Tip Bryozoa. Mshanki, in Khalfin, L. L., Biostratigrafiya paleozoya Sayano-Altaiskoi gornoi oblasti, v. 1, Nizhnii paleozoi: Sibir. Nauchno-Issled. Inst. Geologii, Geo-

fizikii Mineral'nogo Syr'ya Trudy, v. 19, p. 393-400, pls. 0-14 - 0-16.

QUARTZ-LEACHED GRAPHIC-GRANITE FROM

MONTICELLO, GEORGIA

By

Charles A. Salotti and Vincent Matthews III
Department of Geology
The University of Georgia
Athens, Georgia 30601

ABSTRACT

Quartz-leached graphic granite occurs within one of the zoned pegmetites in the Monticello pegmatite district, southwestern Jasper County, Georgia. The residual feldspar is a dull pale pink maximum microcline. This microcline is generally unaltered but some microcline-void surfaces are coated with a thin layer of low albite and minor amounts of pale-green 3T muscovite.

Graphic-granite from which quartz has been removed occurred sparingly within one of the pegmatites in the Monticello pegmatite district, southwestern Jasper County, Georgia. All of the specimens were found on the dump. However, the mining operation used in these pegmatites is such that their position on the dump was only a few tens of feet at most from their position in the pegmatite.

Most of southwestern Jasper County is underlain by intimately mixed quartzo-feldspathic and hornblendic para- and orthogneiss. These gneisses in general strike to the northeast and have nearly vertical dips. This metamorphic unit is intruded by a norite complex in which the mineralogic and textural banding strikes east-west and dips 55-60° to the north. Large pegmatites up to 400 feet in length intrude the noritic rocks and except for a few small marginal pegmatites are confined to the norite. These pegmatites have a general north-south strike and dip steeply to the west. Most of the pegmatites are zoned, but none has a replacement unit.

The large pegmatite that contained quartz-leached graphic-granite is exposed one mile east of the Gladesville fire tower. The pegmatite is zoned with a granitic textured wall zone of relatively fine-grained quartz and microcline. This zone is generally less than two feet thick. The intermediate zone of graphic-granite occupied most of the pegmatite. Vitreous to slightly milky quartz masses up to two feet in diameter are scattered among the dump rocks and their volume suggests that the quartz core was very small. Locally parts of this core can still be seen in place, and their distribution indicates that the core

Figure 1. Specimen of quartz-removed graphic
granite from Jasper County, Georgia. The en-
tire specimen is unaltered pale-pink maximum
microcline.

was not continuous.

Graphic granite exposed in the walls of the pit is variable in the
degree of development of the graphic texture and also in regard to color
of the microcline. This color varies from white to reddish pink with
most of the microcline being pale pink. X-ray and optical parameters
of all of the microcline color varieties correspond to what Wright and
Steward (1968) defined as maximum microcline. Graphic granite that
has had the quartz removed is invariably a dull pale pink color.

The degree to which quartz has been removed varies from
specimens in which only a slight separation is visible between micro-
cline and quartz to specimens in which all traces of quartz have been
removed. In a fist-sized fragment one side of the specimen has all of

186

the quartz removed, whereas on the opposite side the quartz remains untouched.

The lining of the voids varies from sharply defined walls that still show the twin striations of the removed quartz to irregularly lined voids in which the walls have a "fused" almost botryoidal texture. The walls of the sharply defined voids are unaltered microcline; the walls of the irregular voids are coated with a thin layer of low albite and minor amounts of fine-grained 3-T muscovite. Rarely the well-defined walls have slightly coarser-grained flakes of 3-T muscovite adhering to them. Some voids are irregularly filled with kaolin and very fine-grained quartz. The location and appearance of the latter specimens clearly indicate that these minerals were emplaced in the voids after mining and are surficial in origin.

Several similar occurrences of quartz-removed graphic granite have been reported. Bygden (1904) agreed with Hogbom (1898) that the quartz-removed graphic granite from Skarpö, a neighboring island to Ytterby, had formed by the removal of quartz from normal graphic granite. Schaller (1942) presented a paper entitled, "An unusual specimen of graphic granite" at the 22nd Annual Meeting of the Mineralogical Society of America. His abstract read as follows:

> "In a specimen of graphic granite from New Hampshire the quartz has been completely removed without any change in the microcline. Three similar specimens have been found in California.
>
> From specimens found in Maryland only a little quartz has been removed."

Schaller did not publish further on any of the occurrences.

The Skarpo and the Georgia pegmatites have a number of common features including the following: 1) both are zoned pegmatites without replacement units; 2) well-developed graphic granite constitutes an unusually large volume of both pegmatites; 3) both have a simple mineralogy of microcline, quartz and lesser amounts of Na-plagioclase; and 4) quartz-removed graphic granite comprises a small part of the total pegmatite.

The Skarpo and Georgia deposits differ in at least two important respects. First, at Skarpo, to quote Hogbom (1898), "The graphic structure with respect to quartz as well as those with cavities occurs in both feldspars, more beautiful and more frequent, however, in the microcline." The quartz-removed graphic granite in Georgia is confined to microcline. Secondly, at Skarpo some of the cavities are lined with orthoclase and rarely filled completely with orthoclase. Hogbom (1898) describes these orthoclase fillings as, "... uniformily oriented to microcline...". A secondary coating of the cavities is uncommon in the Georgia occurrence and is confined to cavity walls in the more irregular cavities. This secondary coating is low albite in the Georgian occurrence.

187

Because the minerals present are rock-forming species, this unusual graphic granite is intriguing beyond its interest as a mineralogical curiosity. Hogbom (1898) hypothesized that quartz was removed before crystallization was complete and, "The orthoclase veneer of the cavities is likely the latest crystallization product of the feldspar substance". Considering the likelihood of equilibrium or close to equilibrium conditions prevailing in the interior of a forming igneous pegmatite, and the experimental evidence pertinent to the system, $NaAlSi_3O_8$ - $KAlSi_3O_8$ - SiO_2 - H_2O, it is difficult to envision a crystallization path that would result in quartz-removed graphic granite surrounded by unaltered normal graphic granite.

On the other hand if removal were post solidification, the questions arise as to the conditions and what type of solvent can remove quartz without effecting the enclosing feldspar and, even granting solution is possible, what happened to the removed silica.

Clearly the origin of quartz-removed graphic granite is a part of the larger problem of the origin of cavities in pegmatitic bodies. On the basis of our observations of the Georgia specimens we can propose no new theories. It has been our intention in this note only to point out another occurrence of quartz-removed graphic granite and to briefly discuss its relation to the previously described sample from Skarpö, Sweden.

REFERENCES

Bydgen, A., 1904, Uber das quantitative Verhaltnis zwischen Feldspat und Quarz in Schriftgraniten: Bul. Upsala Univ. Geol. Inst. v. 7, p. 1-18.

Hogbom, A. G., 1898, Ueber einige Mineralverwachsungen: Bull. Upsala Univ. Geol. Inst., v. 3, p. 433-453.

Schaller, Waldemar, 1942, An unusual specimen of graphic granite: Am. Mineral, v. 27, p. 233.

Wright, T. L., and Stewart, D. B., 1968, X-ray and optical study of alkali feldspar: I. Determination of composition and structural state from refined unit cell parameters and 2V: American Mineral., v. 53, p. 38-88.